Chapter 8: System Identification and Modeling of Key Actuator Properties

Based on experimental findings presented in previous chapters, polypyrrole actuators exhibit the following properties:

- At low frequencies, and long times, the impedance is capacitive, with the capacitance being on the order of 10^7-10^8 F·m^{-3}.
- At high frequencies the impedance appears to be primarily resistive.
- The polymer exhibits visco-elastic behavior, with a stiffness immersed in electrolyte, of $E \sim 0.6$ GPa.
- Strain is proportional to charge transferred, relatively independent of load to >30 MPa, via a strain to charge coefficient, $\alpha \sim 1\times10^{-10}$ m^3·C^{-1}. Equivalently, the stress is proportional to charge at fixed length, via the constant of proportionality $\alpha \cdot E$, such that: $\varepsilon = \frac{\sigma}{E} + \alpha \cdot \rho$, where ρ is the charge per unit polymer volume.
- Strain appears to be diffusion limited at intermediate frequencies.
- The impedance appears to be linear (i.e. obeys scaling and superposition) over a range of applied potentials of several volts over short periods, and of about 1 V at long times.
- Strain rate and power to mass are increased by applying shaped potentials that compensate for electrolyte resistance.

- The polymer has a high electrical conductivity, σ=1-4×10^4 S·m^{-1}.

These observations are now incorporated into a model that explains and predicts conducting polymer performance. The model predictions are then compared with experimental results obtained from swept sine linear system identification techniques. The model and the experimental results provide insight into a number of important questions: What are the physical mechanisms responsible for electrical to mechanical energy transduction? What performance can be obtained currently, and what are the ultimate stresses, strains, power to mass ratios and efficiencies that can be expected? Is it possible to develop analytical models of actuator response such that a designer can predict behavior under a variety of conditions and optimize the actuator configuration of meet performance specifications?

Chapter 8 presents a combined physically-based/empirical theory that explains and predicts the relationship between inputs (voltage/charge) and outputs (stress/strain). An analytical expression results, which relates the stress, strain, strain rate, power to mass and electrical to mechanical energy conversion efficiency to current or voltage input, given polymer dimensions, the electrolyte and contact resistances, the double layer capacitance at the electrolyte-polymer interface, the ionic diffusion coefficient within the polymer, and the strain to charge ratio. In the model, known as the diffusive-elastic-metal model, the polymer is treated as a three dimensional electrochemical capacitor, which is charged and discharged via the diffusion of ions from the adjacent electrolyte. Alternative models are also presented, and their predictions discussed.

Chapters 9 and 10 describe the experimental apparatus employed, and present the results obtained from linear system ID. For each polymer strip the electrical admittance and the

transfer function between strain and current at constant stress are measured. In some films the transfer function relating stress and current and the stress/strain relationship are also recorded. The model is fit to the admittance data to obtain estimates of the ionic diffusion coefficient for dopants within the polymer matrix. The strain to charge ratio is estimated from the strain to current data. From these, strain rate, power to mass, and efficiency are calculated and modeled.

8.1 Polymer Electro-mechanical Modeling: The Diffusive-Elastic 'Metal'.

In order to understand the ultimate performance limits of conducting polymer actuators, and to predict their response for design purposes, it is important to have models that describe actuator behavior, and provide physical insight into the underlying physical mechanisms of electro-mechanical coupling. The aim is to describe and preferably understand the process of electrical to mechanical energy transduction. In this chapter a model is proposed, in which the actuator is treated as an electrolytic capacitor with the unusual feature that charging occurs throughout its volume. The rate of charging is limited by the rate of ionic diffusion into the polymer. An expression for electrical admittance is derived, which, when combined with the assumption of a fixed proportionality between strain and charge, enables the prediction of stress, strain, strain rate, power to mass and efficiency as a function of input voltage or current and the applied load. Other candidate models are also put forward, and their predictions compared. Subsequent chapters then compare model predictions with experimental results.

8.2 Background

In previous chapters, experimental results presented suggest that:

- Polymer expansion is associated with ion insertion;
- Strain is directly proportional to charge and independent of stress up to 30 MPa or more;

- At long times (after several hundred seconds), voltage is proportional to the charge transferred over a range of ~ 1V;
- At short times (< 10 ms) the current is proportional to applied potential;
- Superposition and scaling of between input voltage and output current are observed;
- The magnitude of strain as a function of time/frequency suggests that diffusion is a rate-limiting factor.

These results suggest that a linear, time-invariant model is suitable to describe both the relationship between current and voltage (admittance) and between current/voltages and stress/strain. Furthermore, the impedance should look purely resistive at high frequencies, be diffusion limited at intermediate frequencies, and appear capacitive at low frequencies.

The proposed mechanisms involved in polymer charging are outlined in Figure 8.1 (a) through (d), which depicts a polymer electrode, an electrolyte phase and a counter electrode to each side of the polymer. Potential between the polymer and a reference electrode is set via a potentiostat. It is assumed that only anions are able to penetrate into the polymer, due to their smaller size. The application of the theory to the case of small cations and excluded anions, both ions excluded or only anions excluded is straightforward.

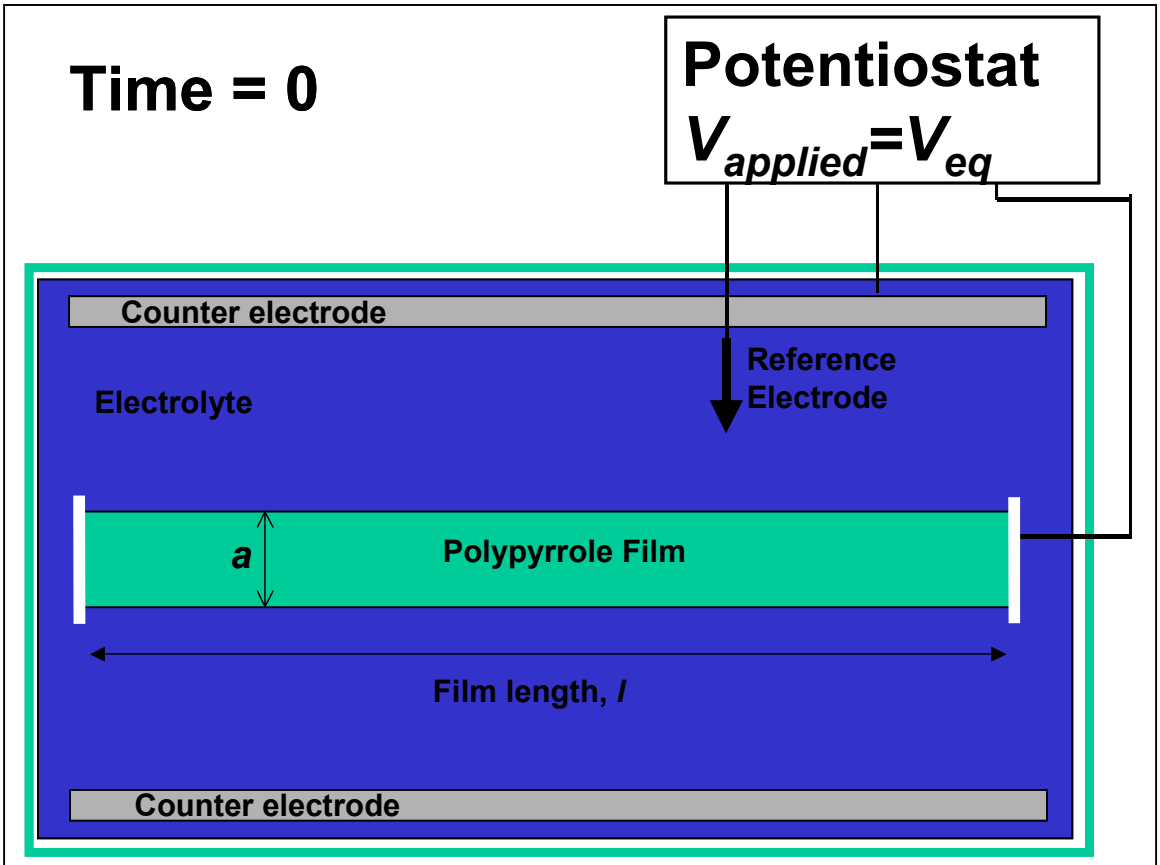

Figure 8.1: Model of polypyrrole charging and Swelling. (a) A polypyrrole film of thickness, *a*, immersed in an electrolyte containing small anions and bulky cations that cannot penetrate the polymer, is at equilibrium, at an applied voltage, V_{eq}.

When a voltage is applied between the reference and the working electrode, Figure 8.1(b), ions within the electrolyte are transported by electrophoretic force, with anions and cations traveling parallel to the applied field and in opposite directions. The initial impedance is resistive in nature, and no changes in strain or stress are expected in the polymer. As depicted in Figure 8.1(c), these charges concentrate at the polymer/electrolyte interface. As the ions approach the interface, the polymer surface charges electronically, thereby preventing electric field from penetrating the polymer surface. The ions and charges form what is known in electrochemistry as a double layer capacitance. The spacing between ions and electronic surface charges, δ, is typically less

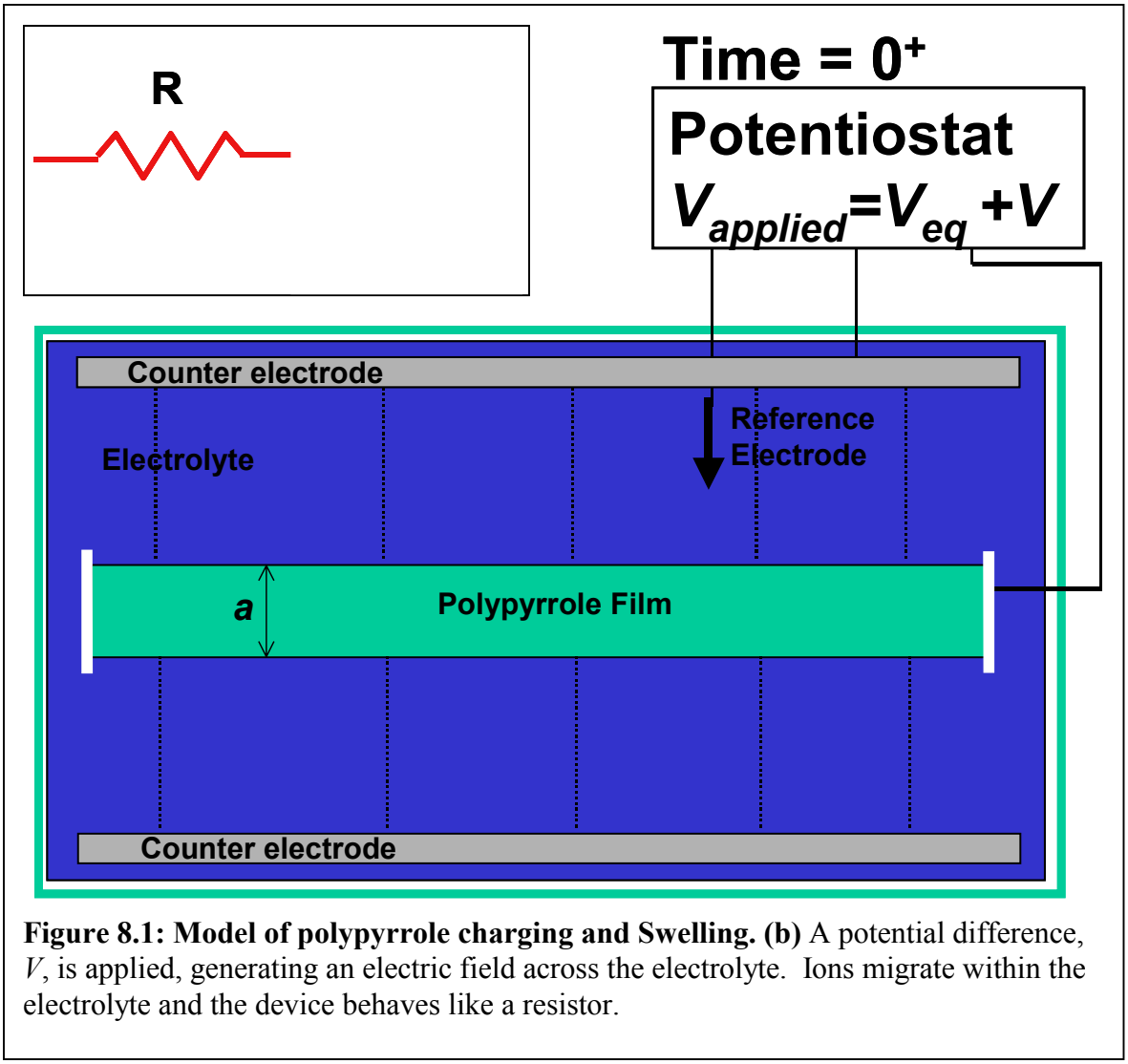

Figure 8.1: Model of polypyrrole charging and Swelling. (b) A potential difference, *V*, is applied, generating an electric field across the electrolyte. Ions migrate within the electrolyte and the device behaves like a resistor.

than 30 nm in electrolytes of moderate concentration, leading to very strong fields with typical capacitances (Bull, Fan and Bard 1982) of between 0.1 and 0.4 $F \cdot m^{-2}$. The polymer is assumed to have a much lower electronic resistance than the ionic resistance of the electrolyte and the field at its surface is assumed to be uniform, such that charging is uniform.

The polymer is assumed to be porous at the molecular scale, enabling ions and solvent of sufficiently small size to enter and leave. The electronic conductivity of the polymer prevents fields from arising within the polymer, and thus, unlike in the electrolyte, there

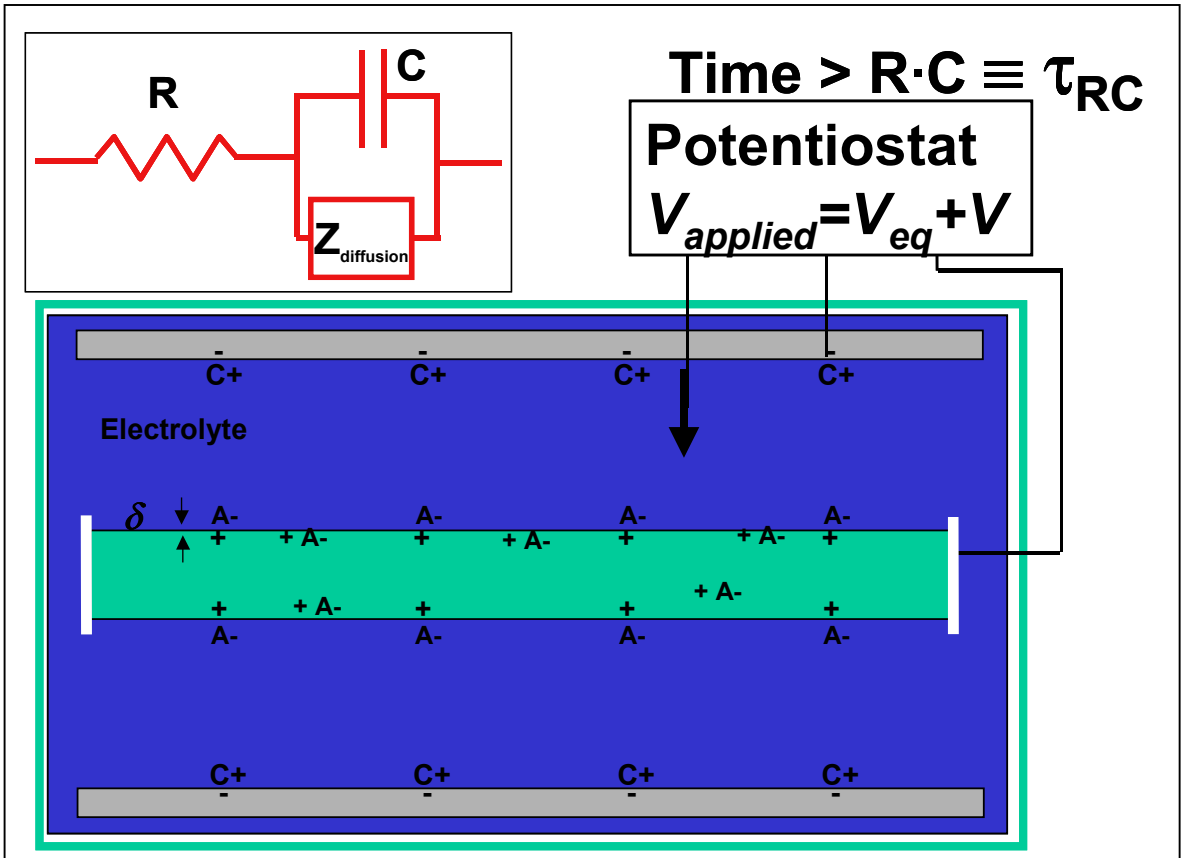

Figure 8.1: Model of polypyrrole charging and Swelling. (c) The migration of anions, **A-**, and cations, **C+**, leads to a build-up of ionic charge over a distance, ***δ***, at the polymer/electrolyte interface, balanced by electronic charge, +, and forming a double layer capacitance, **C**. Some anion/charge pairs diffuse into the polymer, discharging the double layer and swelling the polymer.

is no electrophoretic force on ions, and convection is not possible, so any dopant transport must occur by diffusion.

The potential difference at the polymer/electrolyte interface makes the insertion or removal of dopant/charge pairs energetically favorable. The energetics of insertion is assumed to be capacitive in nature, with the number of charges inserted proportional to the change in double layer potential. The dopant flux alters the concentration of dopant/charge pairs at the polymer surface, creating a concentration gradient within the material, which, in turn, leads to diffusion of ion/charge pairs into the polymer, Figure

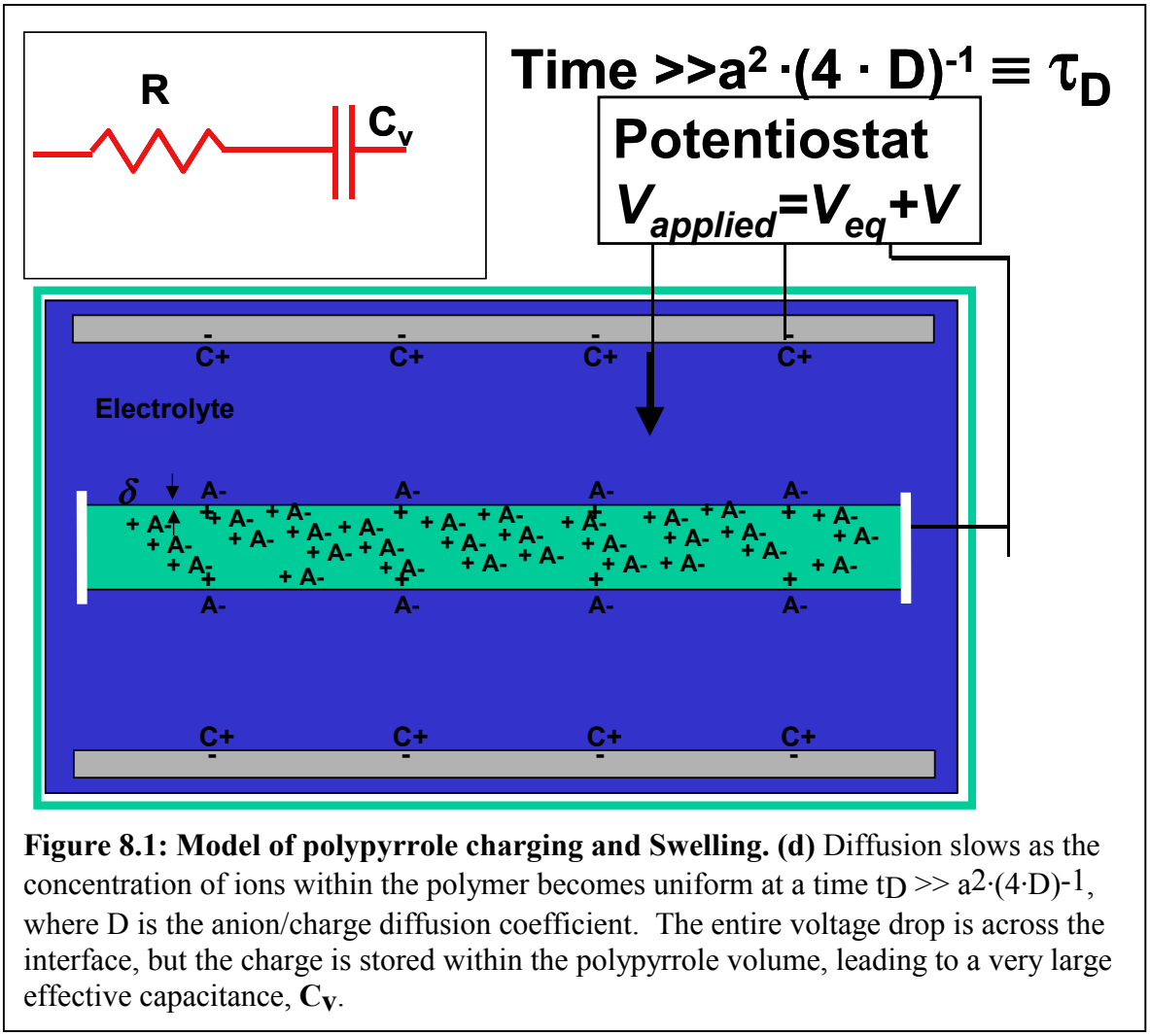

Figure 8.1: Model of polypyrrole charging and Swelling. (d) Diffusion slows as the concentration of ions within the polymer becomes uniform at a time $t_D >> a^2 \cdot (4 \cdot D)^{-1}$, where D is the anion/charge diffusion coefficient. The entire voltage drop is across the interface, but the charge is stored within the polypyrrole volume, leading to a very large effective capacitance, $\mathbf{C_V}$.

8.1 (c). Strain rate is assumed to be directly proportional to the diffusion current. Thus, at short times/ high frequencies, strain rate is high, but drops over time, as concentration gradients are reduced. Eventually, diffusion currents permeate the entire polymer, the concentration becomes uniform and diffusion ceases, Figure 8.1 (d). The polymer is fully charged or discharged, and the full strain has been achieved for the given change in voltage.

The model provides qualitative explanations for all of the observations. At high frequencies and short times the behavior is resistive, owing to the solution resistance. At longer times, the double layer begins to charge and ions diffuse into the polymer.

Current and strain rate are controlled by the rate of diffusion, and the extent of double layer charging. At long times, the thermodynamics determine the state, producing a capacitive response, and strain proportional to applied potential. The quantitative predictions are now investigated.

8.3 Theory

The equations representing the diffusive-elastic-metal model are now derived. The model name stems from the assumptions that mass transport is limited by molecular diffusion within the polymer, that the polymer expands in response to ion insertions in an elastic manner, and that the polymer has a negligible electronic resistance compared to the rest of the cell, and is thus metal-like. The mechanisms of polymer electronic conduction need not be truly metallic in nature.

8.3.1 Assumptions

The challenge is now to represent the phenomena mathematically. The configuration to be modeled is as shown in Figure 8.1. A strip of polymer has a length, l, a width, w, and a thickness, a, in contact with an electrolyte over a surface area $A=2\times w\times l$, and is mechanically connected at each end. It is assumed that $w>>a<<l$. The mechanical connections either provide a constant force (isotonic condition) or sit a fixed distance, l, apart (isometric condition). Electrical contact is also made with the polymer. Voltage is applied and measured relative to an ideal voltage source also in the electrolyte (in practice provided by a combination of a reference electrode and a potentiostat). Furthermore, several assumptions are made about the nature and properties of the polymer and the electrolyte:

1. The polymer is porous, allowing ions and molecules to diffuse within it;
2. Convection and migration of ions and solvent within the polymer are negligible, (contradicting several models, as is discussed below);
3. Electrical contact with the polymer is characterized by a contact resistance, R_c. This resistance represents the electrical impedance arising from contact between the polymer and a metal electrode used to make electrical contact between the polymer and the potentiostat;
4. Potential drops within the polymer are negligible compared with the applied reference to polymer voltage difference;
5. The impedance of the electrolyte is characterized by a resistance, R_s. Effects of ion depletion near the polymer interface are considered to be negligible, since mass transport in the polymer is assumed to be much slower than in the electrolyte;
6. The double layer capacitance, C, is described by a parallel plate model, with surface area, A, dielectric constant, k and separation, δ;
7. The internal capacitance per unit volume of the polymer is equal to the double layer capacitance per unit volume, $C \cdot A^{-1} \cdot \delta^{1}$, for reasons discussed below;
8. No electron transfer (Faradaic reaction) takes place between the electrolyte and the polymer;
9. The polymer mechanical constitutive relations are assumed to be linear elastic, with strain, ε, directly proportional to the extent of polymer charging, ρ, at

constant stress, σ. All strains are assumed to be small and creep/stress relaxations are neglected. Stiffness is assumed to be independent of oxidation state;

10. Negligible mechanical coupling exists between the polymer and the electrolyte;

11. Only a small part of the total electrical energy input creates mechanical work; and

12. All processes are linear and time invariant.

These assumptions will not hold when the polymer is in an insulating state, and thus only apply over a limited potential range. In 11, it is assumed that the electrical impedance can be modeled without regard for the coupling to mechanical energy being expended. Number 7 implies that not only are the energies per charge in the double layer and within the polymer the same, as required by thermodynamics*, but so is the second derivative of energy with respect to charge. Why should the double layer capacitance be so closely tied to the volumetric capacitance? Double layer charging is the surface manifestation of the effect of inserting charge within the polymer, so there is no doubt that the physics of the two situations are related. There is also a large solvent content within the polymer, in the case of PPy(PF_6^-)† in propylene carbonate, providing a similar dielectric environment. However, there is also a clear anisotropy at the polymer surface that is not present within the bulk. How this manifests itself will depend largely on the relative placement of charges, and solvent molecules. The symmetry of the two cases suggests that the ratio of

---

* Interactions between particles both within the polymer and the double layer are assumed to determine the population of states, with entropy playing a minimal role. The presence of very strong electrostatic forces and the capacitive behavior observed over potential ranges of more than 1 V are used to justify this assertion in further discussions below.

† Represents polypyrrole doped with hexafluorophosphate anions used in this study.

bulk to surface capacitance will be between 1 and 2. As a first modeling attempt, the capacitances are assumed equal, thereby reducing the model complexity by one parameter, and requiring that changes in ion concentration at the double layer be matched one to one in the polymer. The assumption is tested by direct measurements of double layer capacitance. Future refinements may involve adding a factor to account for the differences in capacitances.

Several of the assumptions are not in agreement with models and results that are presented in the literature. These models and results are discussed in more detail at the end of this chapter, and differences in predicted behaviors are listed, which are then compared with experimental findings in subsequent chapters.

8.3.2 Model derivation: The Diffusive-Elastic 'Metal'.

The current in response to a step change in voltage between the polymer and the reference electrode is now determined, from which the admittance transfer function (inverse of the impedance) is obtained. Next the strain in response to applied current/voltage is determined, and finally an expression is derived for the electrical to mechanical efficiency.

The electrolyte and metal-polymer contact act as a resistance, $R=R_c+R_s$, and the interface between the polymer and the electrolyte as a double layer capacitance, C. Current, I, passing though the cell must traverse the electrolyte. The current charges the double layer capacitance, which is simultaneously discharged by diffusion of ion/electronic carrier pairs into the polymer. Diffusion is driven by concentration gradients, whereas

ionic currents and double layer charging are driven by potential gradients. These 'forces' are now related, and an expression for the admittance, Y, is obtained in terms of :

- Circuit resistance, $R=R_s+R_c$,
- Double layer capacitance, C,
- Polymer thickness, a,
- Polymer surface area, $A=2\times w\times l$,
- Coefficient of ionic diffusion in the polymer, D,
- Double layer separation, δ,
- and the Laplace variable, s.

Intermediate variables and constants include:

- the double layer charging current, I_c,
- the diffusion current, I_D,
- the ionic concentration within the polymer as a function of position and time, $c(x,t)$,
- and the Faraday constant, $F = 9.64846\cdot 10^4$ Coulombs per mole.

Figure 8.2 is a schematic of the model circuit, including Z_D, the diffusion impedance for a film of finite thickness.

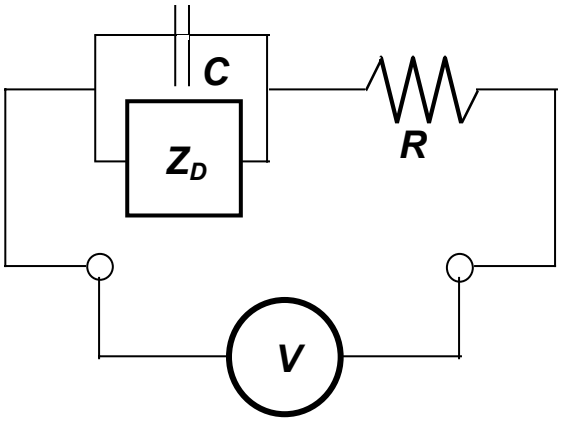

Figure 8.2: Equivalent circuit model of the actuator impedance. *V* represents an external voltage source, *C* the double layer capacitance, *R* the electrolyte/contact resistance, and Z_D, the diffusion impedance.

The total cell current, *I(t)*, is the sum of the diffusion and double layer charging currents:

$$I(t) = I_C(t) + I_D(t), \tag{1}$$

and the total potential drop is:

$$V(t) = I(t) \cdot R + \frac{1}{C} \cdot \int_0^t I_C(t)dt\,. \tag{2}$$

The diffusion current, I_D, at the polymer/electrolyte interface is given by Fick's first law:

$$I_D(t) = -F \cdot A \cdot D \cdot \left.\frac{\partial c}{\partial x}(x,t)\right|_{x=0}, \tag{3}$$

where *x* is position within the polymer, with *x*=0 at the polymer/electrolyte interface, and *x* increasing normal to the interface and into the polymer. The double layer charging current is:

$$I_C(t) = F \cdot A \cdot \delta \cdot \left.\frac{\partial c}{\partial t}(x,t)\right|_{x=0}. \tag{4}$$

In this last equation the double layer is described as having a thickness, δ, and an area, A, in which the average ionic concentration is varying in time.

One more equation is required, which must relate concentration gradient at the interface to the time rate of change in concentration. The relationship between the two is obtained by convolving the response to a step change in concentration at the boundary with the rate of change in surface concentration. The concentration profile as a function of time, in a film of thickness, a, in response to a step change in concentration, c_o, at x=0 and x=a, is:

$$\frac{c(x,t)}{c_o} = \left[1 - \frac{4}{\pi} \cdot \sum_{n=0}^{\infty} \frac{\sin(\pi \cdot (2 \cdot n + 1) \cdot x \cdot a^{-1}) \cdot \exp(-\pi^2 \cdot (2 \cdot n + 1)^2 \cdot D \cdot t \cdot a^{-2})}{2 \cdot n + 1} \right] = B(x,t) \quad . 5$$

To obtain this result, the initial concentration profile (constant concentration across the film, zero at the edges) is expanded as a Fourier series. Separation of variables is employed to solve the one-dimensional diffusion equation given the boundary and initial conditions.

Next, the superposition principle is applied in the form of the convolution integral such that the concentration profile can be obtained for a nearly arbitrary choice of boundary concentrations with time:

$$c(x,t) = \int_0^t \frac{\partial c(0, t-\tau)}{\partial \tau} \cdot B(x,\tau) d\tau \quad . \qquad 6$$

The use of the step response rather than the impulse response in the convolution integral eliminates the appearance of troublesome singularities later in the derivation.

According to Fick's First Law, the diffusion current is proportional to the gradient in concentration, which, at x=0 (or equivalently x=a) is:

$$\frac{\partial c}{\partial x}(0,t) = -\frac{4}{a} \cdot \int_0^t \frac{\partial c(0,t-\tau)}{\partial \tau} \cdot \sum_{n=0}^{\infty} \exp\left(\frac{-\pi^2 \cdot (2 \cdot n+1)^2 \cdot D \cdot \tau}{a^2}\right) \cdot d\tau . \qquad 7$$

This system of equations (1,2,3,4,7) is transformed into the Laplace domain:

$$I(s) = I_C(s) + I_D(s) , \qquad 8$$

$$V(s) = I(s) \cdot R + \frac{1}{s \cdot C} \cdot I_C(s) , \qquad 9$$

$$I_D(s) = -F \cdot A \cdot D \cdot \frac{\partial c}{\partial x}(x,s)\bigg|_{x=0} , \qquad 10$$

$$I_C(s) = F \cdot A \cdot \delta \cdot s \cdot c(0,s) , \text{ and} \qquad 11$$

$$\frac{\partial c}{\partial x}(0,s) = -\frac{4}{a} \cdot c(0,s) \cdot s \cdot \sum_{n=0}^{\infty} \frac{1}{s + \frac{\pi^2 \cdot (2n+1)^2 \cdot D}{a^2}} . \qquad 12$$

Solving for the admittance, $Y(s)$, as a function of the Laplace variable, s, the material thickness, a, the diffusion coefficient, D, the electrolyte and contact resistance, R, the double layer capacitance, C and the double layer thickness, δ, yields:

$$Y(s) \cdot R = \frac{1}{1 + \frac{1}{R \cdot C \cdot s \left[1 + \frac{4 \cdot D}{a \cdot \delta} \cdot \sum_{n=0}^{\infty} \frac{1}{s + \pi^2 (2 \cdot n+1)^2 \cdot D \cdot a^{-2}}\right]}} = \frac{I(s) \cdot R}{V(s)} . \qquad 13$$

Making use of the expansion*:

$$\frac{\tanh\left(\frac{1}{2}\cdot\sqrt{\frac{s}{x}}\right)}{4\cdot\sqrt{x\cdot s}}=\sum_{n=0}^{\infty}\frac{1}{s+\pi^2\cdot(2\cdot n+1)^2\cdot x}, \qquad 14$$

leads to the relationship:

$$Y(s)\cdot R = s\cdot\frac{\frac{\sqrt{D}}{\delta}\cdot\tanh\left(\frac{a}{2}\cdot\sqrt{\frac{s}{D}}\right)+\sqrt{s}}{\frac{\sqrt{s}}{R\cdot C}+s^{3/2}+\frac{\sqrt{D}}{\delta}\cdot s\cdot\tanh\left(\frac{a}{2}\cdot\sqrt{\frac{s}{D}}\right)}. \qquad 15$$

In this form there are four parameters to be determined, namely the capacitance, C, the diffusion coefficient, D, the double layer thickness, δ, and the resistance, R. The double layer capacitance, C, can be approximately related to δ by assuming a parallel plate capacitor, of area, A, dielectric constant, k, permittivity of free space, ε_o, and plate spacing, δ:

$$\delta = \frac{k\cdot\varepsilon_o\cdot A}{C}. \qquad 16$$

As discussed in Chapter 3, a parallel plate model of double layer capacitance (Helmholtz plane) generally provides a good approximation (Bull and others 1982) at electrolyte concentrations above 0.1 M in high dielectric constant solvents. The dielectric constant is taken to be that of the electrolyte. Film dimensions are readily measured. The

* The algebra involved in simplifying the preceding equation is tedious and was done with the help of Mathcad 2000 Professional, from MathSoft Inc., Cambridge MA, USA, www.mathsoft.com.

unknowns are now reduced to three: the resistance, R, the double layer capacitance, C and the diffusion coefficient, D.

Experimentally, the resistance, R, is estimated by measuring the current and the potential drop across the electrolyte, to find R_s, and adding the measured contact resistance, R_c. The double layer capacitance is likely in the range of 0.1 to 0.4 $F \cdot m^{-2}$ (Bull and others 1982). Independent measurements of volumetric capacitance can be used to estimate C, via the relationship in assumption 7 above. If the $R \cdot C$ charging time is short compared to the time taken to initiate diffusion into the bulk, $\delta^2 \cdot D^{-1}$, then the capacitance is readily determined from the admittance. This leaves the diffusion coefficient as the one free parameter. The upper bound on the diffusion coefficient is $10^{-10}\ m^2 \cdot s^{-1}$, a typical value for ions in water, and reported diffusion coefficients of various ions in polypyrrole are in the range of 10^{-11} to $10^{-15}\ m^2 \cdot s^{-1}$, obtained by fitting models to impedance data.

Dimensional analysis reveals three time constants that determine the dominant rate limiting process at a given frequency or time:

$\tau_D = \frac{a^2}{4 \cdot D}$, the diffusion time in the polymer, beyond which diffusion is mostly complete, and below which diffusion appear spatially semi-infinite,

$\tau_{RC} = R \cdot C$, the double layer charging time, and,

$\tau_C = \frac{\delta^2}{D}$, the double layer diffusion discharging time. At times less than τ_C diffusion currents are negligible. The time constant τ_C represents the time taken for

dopants to cross the electrolyte-polymer interface, and become incorporated into the polymer, and is thus the minimum diffusion time*. At times shorter than the minimum diffusion time, no polymer strain is observed, because no dopant ions have entered or left the polymer. At times greater than τ_D, diffusion comes to completion. Therefore, any changes in applied voltage or current that take place on longer time scales, will result in a uniform charging of the polymer, and therefore appear capacitive. At times shorter than τ_{RC} the double layer is uncharged, the admittance is due to cell resistance, and no polymer strain is observed.

The admittance may be re-expressed in terms of these time constants:

$$Y(s)\cdot R = s\cdot\frac{\frac{1}{\sqrt{\tau_C}}\cdot\tanh(\sqrt{s\cdot\tau_D})+\sqrt{s}}{\frac{\sqrt{s}}{\tau_{RC}}+s^{3/2}+\frac{1}{\sqrt{\tau_C}}\cdot s\cdot\tanh(\sqrt{s\cdot\tau_D})}. \qquad 17$$

This form of the equation is helpful in describing the predicted frequency response.

Figure 8.3 is a plot of admittance gain and phase, *Y(s)*, as a function of frequency (Bode plot) for several values of the double layer charging time constant, τ_{RC}. In all cases shown, $\tau_D >> \tau_{RC}$ and $\tau_D >> \tau_C$, as is expected experimentally, and C=10^{-6} F. At low

---

* δ can be interpreted as the typical distance by which dopants must 'hop' during diffusion to reach another site of local minimum energy, applicable both within the polymer and at the electrolyte interface. The model estimates $\delta \sim$ 2 nm (Chapter 10), while x-ray diffraction (Nogami, Pouget and Ishiguro 1994) and elemental analysis of dry polymer estimate inter-dopant spacing as ~1.3 nm and ~1.7 nm, respectively. The latter number is calculated from the doping level of ~0.3 found by Yamaura (Yamaura, Hagiwara and Iwata 1988b), which indicates the ratio of monomers to PF_6^- within the polymer, and using the density (1300 kg·m^{-3}) to estimate average PF_6^- spacing.

frequencies and long times (time > τ_D), the three dimensional capacitance, C_V, dominates the admittance. Indeed the limiting admittance as frequency tends to zero is:

$$Y(s) = s \cdot C \cdot (\frac{a}{2 \cdot \delta} + 1) = s \cdot C_V \text{, or in terms of the time constants,} \qquad 18$$

$$Y(s) \cdot R = s \cdot C \cdot R \cdot (\frac{a}{2 \cdot \delta} + 1) = s \cdot \tau_{RC} \cdot (\sqrt{\frac{\tau_D}{\tau_C}} + 1) .$$

Note that the three dimensional capacitance is directly proportional to the double layer capacitance, via the relationship $C_V = C \cdot (\frac{a}{2 \cdot \delta} + 1)$ as set in assumption 7 above. At higher frequencies, the nature of the response falls into several categories.

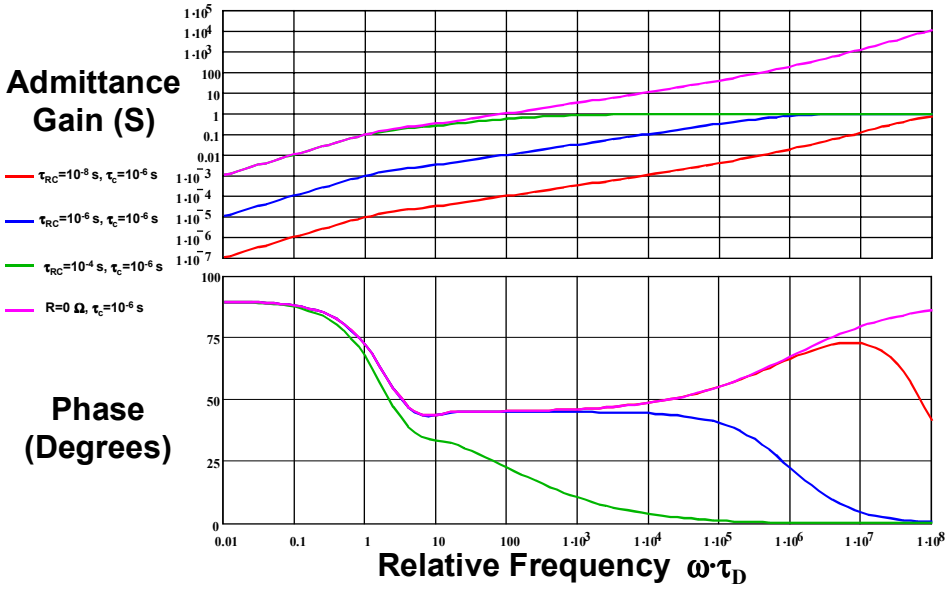

Figure 8.3: The effect of double layer charging time and electrolyte resistance on the admittance of the polymer/electrolyte cell. The resistance, R, is set to 1.0 Ω, except where noted.

Case I: $\tau_{RC} << \tau_C$ (Red Curve in Figure 8.3).

At high frequency, electrolyte and contact resistances dominate the admittance, as is predicted and expected in all cases except when R=0. At frequencies that are lower than the double layer charging frequency, $\tau_{RC}^{-1} > \omega$, but higher than the double layer diffusion discharge frequency, $\omega < \tau_C^{-1}$, the double layer charges fully, and the phase approaches 90º, as the capacitance dominates admittance. Once diffusion is underway, at times > τ_C, or angular frequencies lower than τ_C^{-1}, semi-infinite planar diffusion becomes the rate limiting factor. The Cottrell equation* (Bull and others 1982) tells us that in this case current is proportional to the inverse square root of time, or, equivalently, to the square root of frequency. This square root dependence leads to a 45º phase and a slope of ½. Finally, at low frequencies, with angular frequency, $\omega < \tau_D^{-1}$, the diffusion current penetrates the finite polymer thickness and the entire polymer volume is charged, giving the capacitve response predicted by equation 18. In this low frequency regime, the thermodynamics alone determine the admittance.

Actuation is assumed to occur in response to insertion or removal of charges from the polymer. Thus, actuator bandwidth is set by the minimum diffusion time, τ_C. At angular frequencies below τ_C^{-1}, most of the current is directed to within the polymer, and hence strain rate is limited by the rate of diffusion. Because strain is proportional to the integral of current, the strain amplitude is predicted to increase with decreasing frequency, at a

---

* The Cottrell equation predicts the current, I, as a function of time resulting from planar diffusion into a semi-infinite space: $I = F \cdot A \cdot C \cdot \sqrt{D \cdot t}$ in response to a step change in concentration, C, at a surface of area A. F is the Faraday constant, the charge produced by a mole of fundamental charges.

slope of – ½, until diffusion slows. Below τ_D^{-1}, the diffusion is essentially complete, and the applied voltage, independent of frequency, determines the strain amplitude.

Case II: $\tau_{RC} = \tau_C$ (Blue Curve in Figure 8.3).

When the double layer charging time, τ_{RC}, is equal to the double layer diffusion discharge time, τ_C, the double layer does not fully charge, and therefore the characteristic 90º phase and –1 slope are not observed at high frequency. Planar diffusion dominates in the intermediate frequency regime due to its higher admittance, which has an $\omega^{1/2}$ rather than an ω^1 frequency dependence. Thus the portion of the current passing through the diffusion impedance (Figure 8.2) becomes increasingly large as frequency is reduced, the phase tends to 45 degrees and the slope to ½, until near $\omega = \tau_D^{-1}$, where the finite thickness of the film is relevant, and mass transport is no longer rate limiting. Once again, strain rate is proportional to the admittance at angular frequencies below τ_C^{-1}.

Case III: $\tau_{RC} >> \tau_C$ (Green Curve in Figure 8.3).

Situations in which diffusion discharge of the double layer appears to be much faster than double layer charging until fairly low frequencies are the most commonly observed, as shown in Chapter 10. In this case, the double layer is not able to charge until frequencies that are much lower than τ_{RC}^{-1}, and τ_C^{-1}. As a result, resistance dominates the admittance over a large portion of the frequency range. There is a gradual transition to diffusion-dominated behavior with decreasing frequency, as seen by the slow phase shift from 0º to 45º. Note that the rapid double layer discharge makes it impossible to directly measure the double layer capacitance.

Case IV: R=0 (Magenta Curve in Figure 8.3).

The double layer charges instantly when no resistance is present. At low frequencies the current required to charge the double layer is small compared to the diffusion current, but as frequency approaches the double layer diffusion frequency, τ_C^{-1} the double layer charging increasingly dominates admittance, the slope changes from ½ to 1, and the phase shifts from 45º to 90º. Since strain is proportional to current into the polymer, the model predicts that above τ_C^{-1}, where the diffusion current is negligible, the observed strain will also be negligible. Thus, the diffusion discharge frequency, τ_C^{-1}, is an upper bound on actuator bandwidth.

Achieving zero resistance is equivalent to having a superconducting electrolyte and polymer, an unlikely occurrence. However, it can be recreated to some extent by compensating for voltage drops across the electrolyte and contacts, as is demonstrated in Chapter 7 with the aim of maximizing strain rate. In this technique, the $I \cdot R$ drop is estimated, and added to the voltage output, such that the effective double layer potential drop is held constant.

Summary of Cases

The case analysis shows that at high frequencies the resistance determines the admittance. At intermediate frequencies the double layer charging time, diffusion, or a combination of the two can limit it. The low frequency response is capacitive in nature. Strain rate (at fixed load) is proportional to admittance at frequencies below the maximum diffusion frequency, τ_C^{-1}, where current into bulk of the polymer dominates over surface charging. Strain rate is limited both by diffusion, and by cell resistance.

8.3.3 Discussion and Implications of the Model Admittance

Equations 15 and 16 describe the polymer admittance expected from the diffusive-elastic-metal model. It assumes that the polymer acts as a capacitor whose charging is limited by diffusion and resistance. There are four distinct features that differentiate this new model from those in the literature. First, it accounts for the finite thickness of the polymer, allowing impedance at times both short and long relative to the diffusion time constant, τ_D, to be predicted analytically. Secondly, it includes the effect of electrolyte resistance. Adding electrolyte resistance is easy to do, but is also very important because large diffusion currents can persist even at times much longer than the double layer charging time, τ_{RC}. Thirdly, the double layer capacitance is related to the volumetric capacitance. Finally, it assumes diffusion is due to movement of dopant ions between polymer chains and not through electrolyte filled pores.

A review of the literature shows that several models have been proposed to explain the impedance of polypyrrole in various oxidation states. The most common is the "porous metal" model (Mao, Ochmanska, Paulse and Pickup 1989; Posey and Morozumi 1966). In this model, the polymer is assumed to have supermolecular-sized, electrolyte filled pores. As in the diffusive-elastic-metal model (DEM), the polymer electronic conductivity is assumed to be much higher than the electrolyte ionic conductivity. A change in applied potential leads to a wave of charging as electric field gradually propagates into pores, charging the electrolyte/pore interface in the process. The charging is modeled as a semi-infinite (Bull and others 1982), or finite transmission line

(Posey and Morozumi 1966; Mao, Ochmanska, Paulse and Pickup 1989). The mathematical form produced by the model is a solution to the diffusion equation, making it difficult to distinguish experimentally from a similar model that assumes diffusion through supermolecular-sized pores, and double layer charging of the pore walls (Amemiya, Hashimoto and Fujishima 1993). Low frequency capacitance is a result of pore wall charging. The rate of charging or discharging is a function of electrolyte concentration, since the pores are filled with electrolyte, and the electrolyte conductivity is also a function of ion concentration.

Penner, Martin and Van Dyke (Penner, Van Dyke and Martin 1988; Penner and Martin 1989) propose a model in which changes in conducting polymer oxidation state are limited by the rates of ionic diffusion. Their model is aimed at explaining the rate of change in oxidation state of a neutral, non-electronically conductive polymer undergoing doping. They therefore assume that all electron transfer occurs at the interface between the polymer and the metal electrode in contact with it. The charge transfer is Nernstian, creating a "pseudo-capacitance" in response to small amplitude (10 mV) perturbations. Penner and colleagues also include in their model a resistive term to account for kinetics-limited charge transfer. They treat the limiting cases of semi-infinite diffusion, and steady-state, finite diffusion, but not the transition from one to the other. Their model predicts that polymer capacitance is a function of applied potential, as given by the Nernst equation, and is therefore easily distinguished from the diffusive 'metal'* model.

---

* Whether or not conducting polymers, even those of very high conductivity, can be considered metals is still the subject of debate. The polypyrrole(PF_6) used in this study has finite conductivity down to liquid helium temperatures, and likely below, thereby meeting a minimum requirement.

Ho, Raistrick and Huggins (Ho, Raistrick and Huggins 1980a) propose a model intended to describe the impedance observed during intercalation of ions into electronically conductive and porous electrodes. They assume diffusion limited behavior, and obtain an analytical expression for admittance as a function of frequency in a material of finite thickness. Unlike the diffusive metal model, Ho et. al. assume a Nernstian charge transfer, do not include the effect of electrolyte resistance or surface charging, and add a resistive term in series to account for kinetics.

Finally, it has been proposed that convection in pores may speed mass transport within polypyrrole. In this model(Mazzoldi, Della Santa and De Rossi 1999), convection occurs in response to changes in internal stress resulting from changes in doping state. The model has been applied to explain creep, but it is at least conceivable that the rate of convection of electrolyte in pores could determine admittance. The convection is modeled as a finite transmission line, with resistance to flow along pores and a capacitance within the pore as it is expanded or contracted. Once again, the mathematical form is a solution of the diffusion equation. Methods of distinguishing between models are discussed at the end of this chapter.

What are the implications of the diffusive metal model for actuator design? In previous chapters it is shown that strain rate is proportional to current below the minimum diffusion time, τ_C. The R=0 case, depicted in Figure 8.3, shows the maximum current that can be expected for a given double layer capacitance, applied potential, and diffusion coefficient. Given that strain rate under fixed load is proportional to current, eliminating resistance maximizes strain rate. However, the resistance need not be reduced to zero in order to obtain the maximum strain rates. One approach is to increase the applied

potential. This can be done up to a point, but eventually parasitic reactions will occur, which will decrease efficiency and may irreversibly change the polymer, degrading performance. However it is the double layer potential drop that drives parasitic reactions and not the total potential drop. At high frequencies a large portion of the total drop is across the solution and the contact resistance. By measuring the resistance (i.e. by determining the admittance at high frequency/short times), the proportion of the total potential drop that is across the double layer can be determined. The applied potential can then be increased at intermediate and high frequencies/ short times, such that the double layer potential drop reaches, but does not exceed, a limiting potential. This technique, known in the electrochemical literature as electrolyte resistance compensation, enables the current to be maximized (as given by the R=0 curve), and hence strain rate and mechanical power to mass ratio to be maximized. A drawback of this approach is that electrical to mechanical energy conversion efficiency is reduced. The implementation of this procedure to obtain high strain rates is described in Chapter 7.

What are the implications for efficiency? As an electrostatic energy storage device, the model predicts that the inverse of the diffusion time constant, τ_D^{-1}, sets the bandwidth. At higher frequencies, losses associated with resistance and diffusion reduce the efficiency of electrical energy storage. The efficiency of storage approaches 100 % for operation at angular frequencies of less than τ_D^{-1}. If the efficiency of electrical energy storage is close to 100 %, where is the energy to perform mechanical work? A limitation of the model is clear – there is no pathway for electrical to mechanical energy transduction. It has been assumed that the mechanical coupling is negligible. Data in previous chapters shows that generally less than 1 % of the electrical energy input produces mechanical work.

However, at low frequencies the admittance predicts that all energy input is stored electrically and can be recovered. The issues of mechanical to electrical coupling are now presented.

8.3.4 Electro-Mechanical Coupling

The relationship between electrical input and mechanical output is central to the performance of conducting polymers actuators. As a first step, the induced strain is assumed to be proportional to the charge transferred. Electrical to mechanical conversion efficiency is predicted from this initial model, which further assumes that in general the mechanical energy created is small compared to the electrical energy input. Using this assumption allows Equation 15, the admittance expression, to be used to relate current and voltage in calculating efficiency, as it assumes that electrical to mechanical coupling is negligible. The latter assumption is shown to be generally valid, apart from at low frequencies where the model admittance becomes largely capacitive, and hence no energy is dissipated, and at very high applied loads, where mechanical work becomes significant. Admittance is modified to take electro-mechanical coupling effects into account. Finally, predictions are made as to the efficiency of conducting polymers as electrical generators.

8.3.4.1 Electro-mechanical Coupling

Strain, ε, is assumed to be proportional to charge per unit volume, ρ, via the strain to charge coefficient, α, such that $\varepsilon = \alpha \cdot \rho$. In the Laplace domain, given a polymer of volume, V_f, the relationship between current and strain is:

$$\varepsilon(s) = \frac{\alpha \cdot I(s)}{s \cdot V_f}. \qquad 19$$

The strain to current transfer function is therefore very simple in form, the gain having a slope of –1 and the phase an angle of –90 degrees. This relationship only applies at angular frequencies below the maximum diffusion frequency, $\tau_C^{-1}=D\cdot\delta^2$, where most of the charge is related to diffusion of ions into the polymer matrix, rather than surface charging.

Equation 19 is empirically derived. However, it provides some insight into the underlying mechanisms responsible for electro-mechanical coupling. Consider a polymer matrix that expands isotropically, with small deformations. The change in volume per unit charge density is:

$$\frac{\Delta V_f}{V_f\cdot\rho}=\frac{3\cdot\varepsilon}{\rho}=3\cdot\alpha\,. \qquad 20$$

Thus $3\cdot\alpha$ provides a measure of change in volume induced per unit charge, and is observed to be ~1.5×10^{-10} $m^3\cdot C^{-1}$ for polypyrrole doped with hexafluorophosphate in propylene carbonate. Expressed in terms of elementary charge, the volume change is 7×10^{-29} m^3 per charge transferred, or 0.07 nm^3. A sphere of equivalent volume has a diameter of between 0.5 and 0.6 nm. The diameter* of the PF_6^- anion is roughly 0.5 nm. This observation suggests that the strain to charge ratio, α, is directly proportional to dopant ion volume. Interestingly, the strain to charge ratio observed in a

* Van der Waals diameters are estimated from CambridgeSoft's CS Chem3D Pro Version 4.0, © 1997, www.chemoffice.com.

tetraethylammonium hexafluorophosphate solution in water is roughly double, as shown in Chapter 5*.

The electrical to mechanical conversion efficiency can now be determined in terms of the admittance and the strain to charge ratio. Efficiency is the ratio of mechanical work done to electrical energy input. The electrical energy expended, w_e, in a given time, T:

$$w_e = \int_{t=0}^{T} V(t) \cdot I(t) \cdot dt , \qquad 21$$

and the mechanical work, w_m, is:

$$w_m = V_f \cdot \int_{0}^{T} \sigma \cdot d\varepsilon = \int_{0}^{T} \sigma \cdot \alpha \cdot I(t) \cdot dt . \qquad 22$$

The efficiency is thus:

$$e = \frac{\int_{t=0}^{T} \sigma \cdot \alpha \cdot I(t) \cdot dt}{\int_{t=0}^{T} V(t) \cdot I(t) \cdot dt} . \qquad 23$$

From expression 23 it is easy to see that the efficiency in response to a step voltage input at constant load is:

$$e = \frac{\sigma \cdot \alpha}{V} . \qquad 24$$

This expression predicts that large loads and high strain to charge ratios will maximize efficiency, as will low voltages. The product of the stress and the strain to charge ratio

* It may be that water molecules are entrained with dopant ions. If so, the diffusion coefficient in aqueous

produce a 'mechanical voltage', $V_m=\sigma\cdot\alpha$. This product is 0.15 mV at 1 MPa and 4.5 mV at 30 MPa, given a typical strain to charge ratio of 1.5×10^{-10} $m^3\cdot C^{-1}$ found in Chapters 5 and 10. Applied potentials typically range from 100 mV to 2000 mV, so that, in general the 'mechanical voltage' is less than 5% of the electrical potential, V and the work done is less than 5% of the total electrical energy input. Thus the assumption that mechanical coupling can be neglected in describing admittance, as used in deriving Equation 15, is justified. Furthermore, if polypyrrole actuators in their current forms are to compete with other actuator technologies on the basis of efficiency, some of the input electrical energy will need to be recovered[*]. Note that the expression breaks down at small applied potentials. Modifications to handle the low voltage case are made in the next section.

The next step is to combine the relationship between current and voltage in Equation 15 with the general efficiency expression in Equation 23 to determine efficiency for any input voltage waveform. To do this, efficiency is found as a function of frequency. Finding efficiency for a given waveform is then a matter of integrating the frequency dependent efficiency, weighted by the input power spectrum, and dividing by the total power. Efficiency equations can be derived in the time domain, but, due to the infinite series expansions that arise in converting the admittance Equation 15 to the time domain, involve tedious infinite series that are unwieldy, and therefore more difficult to interpret.

---

electrolyte is expected to be lower than in propylene carbonate.

[*] Efficient energy recovery will require a custom circuit to extract and store electrical energy from the actuator.

At a given angular frequency, ω, over one cycle of period, T, the electrical energy expended is:

$$w_e(\omega) = \int_{t=0}^{T} V \cdot cos(\omega \cdot t) \cdot V \cdot |Y| \cdot cos(\omega \cdot t + \angle Y(i\omega)) \cdot dt = V^2 \cdot Re(Y(i\omega)) \cdot \pi \cdot \omega^{-1},$$

or

$$w_e(\omega) = V^2 \cdot |Y(i\omega)| \cdot cos(\angle Y(i\omega)) \cdot \pi \cdot \omega^{-1}. \quad 25$$

When the admittance phase, $\angle Y$, is 90 degrees, as is predicted for frequencies < τ_D^{-1}, the energy expended per cycle is zero, assuming that stored energy is recovered. At frequencies greater than the inverse double layer charging time, τ_{RC}^{-1}, the phase is zero and all input energy is expended.

In calculating mechanical work, the case of constant load is treated, as it will be compared with experimental results obtained under isotonic conditions, Chapter 10. At constant load, the mechanical work, w, is simply the product of the force and the amplitude of the displacement. This can be expressed in terms of stress, σ, strain, ε, and polymer volume, V_f:

$$w_m = \sigma \cdot \varepsilon \cdot V_f. \quad 26$$

The work done expressed as a function of frequency, and assuming that none of the mechanical energy is converted back to electrical energy, is:

$$w_m = \sigma \cdot \alpha \cdot \int I(t) \cdot dt = \sigma \cdot \alpha \cdot V \cdot |Y(i\omega)| \int cos(\omega \cdot t + \angle Y(i\omega)) \cdot dt = \frac{\sigma \cdot \alpha \cdot V \cdot |Y(i\omega)| \cdot 2}{\omega}. \quad 27$$

Integration is performed over the positive half of the cycle. The electrical to mechanical energy efficiency, *e*, is the ratio of the work performed, *w*, divided by the electrical energy consumed (Equation 25), w_e:

$$e = \frac{2 \cdot \sigma \cdot \alpha}{\pi \cdot |V| \cdot \cos(\angle Y(i\omega))}. \qquad 28$$

This expression makes intuitive sense, as low voltage, high stress and high strain per unit charge all increase efficiency. If none of the electrical energy input is recovered, the efficiency becomes:

$$e = \frac{2 \cdot \sigma \cdot \alpha}{|V| \cdot \gamma(\angle Y(i\omega))}. \qquad 29$$

The γ term accounts for the fact that the amount of energy expended changes depending on the relative phases of the input voltage and the resulting current. Its value ranges from π when the admittance phase is zero, to 1 when the phase is 90º. When the phase is between zero and 90º, γ is given by the expression:

$$\gamma = \frac{\pi}{180} \cdot \cos(\angle Y) \cdot (180 - \angle Y) + \sin(\angle Y). \qquad 30$$

What is the maximum conceivable efficiency obtainable from polypyrrole actuators, without recovering electrical energy? Tensile strengths exceed 400 MPa in stretch aligned conducting polymer fibers (Baughman, Shacklette and Elsenbaumer 1991). Optimistically assuming that the strain to charge ratio does not decrease for such fibers, the 'mechanical voltage' reaches 60 mV, so that the predicted efficiency reaches 24% for a ±1 V applied potential, and is even higher at lower applied voltages. Under such circumstances the assumption that the work performed is a relatively insignificant part of

the total energy input is invalid. (The assumption is used in deriving the admittance expression, Equation 15, and is generally valid because electrical energies are much greater than the magnitude of mechanical work done). This limitation in the model is also apparent for the case in which stored electrical energy is recovered, Equation 26. At low frequencies the modeled electrical behavior is purely capacitive, the phase is 90º, no energy is dissipated, and the predicted efficiency becomes greater than 1. The next section presents an approach for incorporating electro-mechanical coupling into the admittance relationship, so that efficiencies can be estimated at all frequencies.

8.3.4.2 Modified Impedance: The Diffusive-Elastic-Metal

How should the admittance be modified to account for electro-mechanical coupling? Experiments show that there is a link between charge and strain. In a departure from the model presented up to this point, it is now proposed that voltage and stress are related. The relationships derived in this section are not yet experimentally verified. This is because the electro-mechanical coupling forms a relatively small portion of the total input energy. Further experiments are required which investigate low frequency and low voltage electromechanical response. At low frequencies, net external mechanical work done should appear as a reduction in measured phase of the admittance, due to the fact that not all input electrical energy is stored. At low voltages, and high stresses, the work done will be a relatively large fraction of the total energy input, as predicted by Equations 28 and 29, and hence contributions the electro-mechanical coupling contribution will be observable. The equations presented next form a set of predictions used to guide further experimentation.

8.3.4.2.1 Free Expansion

Consider the case of a free-standing polymer film, into which charge is injected in order to induce expansion. No external forces are applied to the polymer. Electrostatic energy is being expended to change polymer dimensions. The molecular mechanisms involved are unclear, and difficult to probe directly due to the relative disorder of the material, and the minor fraction of total input energy converted to mechanical work. A simple model is therefore proposed, namely that the internal forces that must be overcome are the same as those that resist deformation upon the application of an external load, namely:

$$\sigma = E \cdot \varepsilon = E \cdot \alpha \cdot \rho \,, \tag{31}$$

leading to a change in internal mechanical energy density, u_m, of:

$$u_m = \tfrac{1}{2} \cdot E \cdot \varepsilon^2 = \tfrac{1}{2} \cdot E \cdot \alpha^2 \cdot \rho^2 \,, \tag{32}$$

where E is the polymer modulus of elasticity. Similarly, the inclusion of each additional increment of charge into the polymer matrix requires an increased energy that is proportional to the total charge present:

$V = \frac{\rho}{\overline{C}_e}$, so the electrical energy density, u_e, is: (33)

$$u_e = \tfrac{1}{2} \cdot \frac{\rho^2}{\overline{C}_e} \,, \tag{34}$$

where $\overline{C}_e$ is the capacitance per unit volume. The energy is divided between mechanical work and electrostatic charging. The total potential energy density is the sum of the electrostatic and elastic energies:

$$u = \tfrac{1}{2} \cdot \frac{\rho^2}{\overline{C}_e} + \tfrac{1}{2} \cdot E \cdot \alpha^2 \cdot \rho^2 = \tfrac{1}{2} \cdot \rho^2 \cdot \left(\frac{1}{\overline{C}_e} + \frac{1}{\overline{C}_m} \right), \qquad 35$$

where the mechanical 'capacitance' per unit volume is defined as $\overline{C}_m \equiv (E \cdot \alpha^2)^{-1}$. The 'mechanical capacitance', C_m, is in series with an electrical capacitance, C_e, so that the total capacitance is:

$$\frac{1}{\overline{C}} = \frac{1}{\overline{C}_e} + E \cdot \alpha^2 = \frac{1}{\overline{C}_e} + \frac{1}{\overline{C}_m}. \qquad 36$$

The approximate magnitudes of these capacitances can now be estimated by inserting typical values of E (~0.6 GPa), α (~1.5×10^{-10} $m^3 \cdot C^{-1}$), and of the volumetric capacitance obtained from data in Chapters 5 and 10. The mechanical capacitance is expected to be 10^{11} $F \cdot m^{-3}$, while the total volumetric capacitance is on the order of $5 \cdot 10^7$ $F \cdot m^{-3}$, as observed in Chapters 5 and 10. These estimates indicate that the mechanical energy density is ~2000× lower than the 'electrostatic' energy density. Note that these calculations assume that the actuator is operated at low enough frequencies that mass transport does not play a role. Later the effects of mass transport are incorporated.

What are the implications for efficiency? Work is done on the surroundings when the polymer expands. If this work is done against atmospheric pressure, or is used to deform a surrounding material with much greater stiffness than that of the polymer, the work performed is negligible. However, from a matched load (same stiffness), half of the work can be extracted, namely:

$$w = \tfrac{1}{4} \cdot E \cdot \alpha^2 \cdot \rho^2. \qquad 37$$

If the stored energy is not recovered, then the electrical to mechanical efficiency is:

$$e = \frac{\frac{1}{4} \cdot E \cdot \alpha^2 \cdot \rho^2}{\frac{1}{2} \cdot \left[\frac{1}{\overline{\overline{C}}_e} + \frac{1}{\overline{\overline{C}}_m} \right] \cdot \rho^2} = \frac{1}{2 \cdot \left[\frac{\overline{C}_m}{\overline{\overline{C}}_e} + 1 \right]} \approx \frac{\overline{C}_e}{2 \cdot \overline{C}_m} . \qquad 38$$

The predicted efficiency is $\sim 2 \times 10^{-4}$. Thus only 0.02% of the input energy performs mechanical work. An impressive 99.9 % of the input electrical energy must be recovered if a 20 % efficiency is to be obtained. The efficiency is lower than those estimated in the previous section because the film is initially unloaded in this case. The case of a loaded film is now examined.

8.3.4.2.2 Applied load and 'mechanical potential'

In the previous section it is suggested that the capacitance has a mechanical component. Next, consider the case of an applied load. The load creates a stress, σ, within the polymer. If charge is transferred while the load is applied, a change in work density of:

$$\Delta w_m = \sigma \cdot \Delta \varepsilon = \sigma \cdot \alpha \cdot \Delta \rho . \qquad 39$$

In general the work done on an external load resulting from charge-induced swelling is:

$$w_m = \int \sigma \cdot \alpha \cdot d\rho . \qquad 40$$

The applied stress acts as a voltage source, or a 'mechanical potential', V_m, defined as:

$$V_m \equiv \sigma \cdot \alpha . \qquad 41$$

This expression predicts that stress inhibits the insertion of charge, and assists in its removal. The sign of the potential changes as the sign of the strain to charge volume

changes; In other words if the strain is induced by the insertion of cations rather than anions, the sign of V_m is reversed. As discussed in previous sections V_m is expected to be between 0.15 to 4.5 mV in polypyrrole given the range of stresses and strain to charge ratios found. The modified equivalent circuit is shown in Figure 8.4, with the voltage source, V_m, representing stresses applied to or by the system and the source, V, representing an external voltage source.

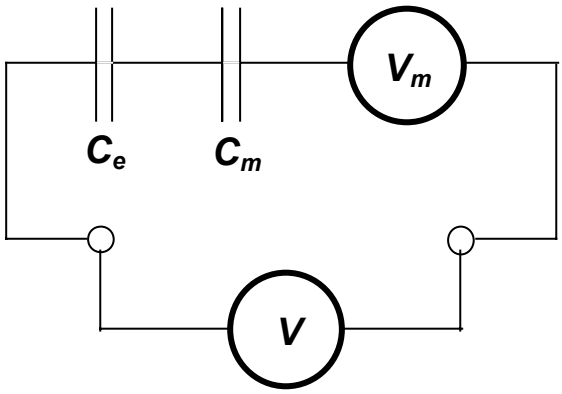

Figure 8.4: Polymer modified electro-mechanical circuit at angular frequencies $< \tau_\Delta^{-1}=D/(2a)^2$. V represents an external voltage source, $V_m=\sigma\cdot\alpha$ an external stress, C_e, stored electrostatic energy, and, C_m, stored mechanical energy.

Note that Figure 8.4 does not include mass transport effects. How can the equivalent circuit in Figure 8.4 be modified to cover time scales shorter than the diffusion time constant, τ_D? The mechanical voltage, V_m represents the additional energy per unit charge required to insert dopants into the polymer as a result of the external load. It therefore belongs in series with the polymer impedance, as shown in Figure 8.5.

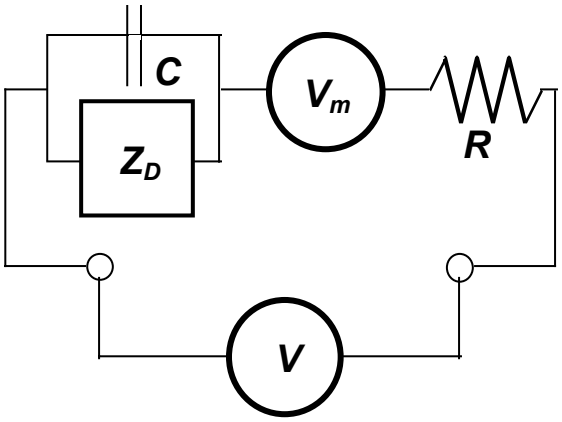

Figure 8.5: Modified polymer/electrolyte equivalent circuit. V represents an external voltage source, V_m an external stress, C the double layer capacitance, R the electrolyte/contact resistance, and Z_D, the diffusion impedance.

Suppose that electrical to mechanical energy transduction is one way, so that mechanical energy input will not result in significant electrical generation. In this case, net mechanical work is done on the surroundings each half cycle. In the load is constant, the work is $w_m = \sigma \cdot \alpha \cdot \rho \cdot V_f = 2 \cdot \sigma \cdot \alpha \cdot Q$, (recall that V_f is polymer volume, Q is charge) and the electrical energy expended is $w_w = \int (V - V_m) \cdot I(t) \cdot dt$. The term involving V has already been solved for as a function of frequency, as shown in Equation 25:

$$w_e(\omega) = V^2 \cdot |Y(i\omega)| \cdot \cos(\angle Y(i\omega)) \cdot \pi \cdot \omega^{-1} = V \cdot \cos(\angle Y(i\omega)) \cdot \pi \cdot Q,$$

where the fact that charge is the integral of current is used to obtain the expression on the right hand side. The V_m term, at constant load, is simply $V_m \cdot Q = 2 \cdot \sigma \cdot \alpha \cdot Q$. The ratio of mechanical work done to electrical energy expended is then:

$$e = \frac{2 \cdot \sigma \cdot \alpha}{|V| \cdot \pi \cdot \cos(\angle Y) + 2 \cdot \sigma \cdot \alpha}. \qquad 42$$

When no electrical energy is recovered, Equation 29 is modified to become:

$$e = \frac{2 \cdot \sigma \cdot \alpha}{|V| \cdot \gamma + 2 \cdot \sigma \cdot \alpha} = \frac{2 \cdot V_m}{|V| \cdot \gamma + 2 \cdot V_m}, \qquad 43$$

where γ is defined in Equation 30, and is between 1 when the admittance phase is 90º and π at 0º. Given an applied voltage of 0.1 V, a load of 15 MPa and a strain to charge ratio of 1.5×10^{-10} $m^3 \cdot C^{-1}$, the predicted efficiency without recovery is 0.05. Note that the efficiency approaches 1.0 as the applied voltage tends to zero, which is not the case in previous expression (Equations 24, 28 and 29).

Increasing applied potential increases strain but reduces efficiency. This is because the insertion of additional charge into the polymer results in a fixed amount of work (given constant stress), but requires an incremental increase in voltage (due to the capactive nature of the impedance). In contrast, if the stress is proportional to strain, then the efficiency is independent of applied voltage, as described by Equation 38.

8.3.4.3 Electrical Generation

Suppose that mechanical energy is input from the surroundings. How much electrical energy can be generated? In the best case, the mechanical energy input equals the electrical energy output over a cycle. The predicted maximum voltage generated is $V_m = \sigma_{max} \cdot \alpha$, is obtained under open circuit conditions, or when the strain is ramped rapidly compared to the $R_{Load} \cdot \overline{C}$ charging time. An upper bound on the voltage is set by the polymer's tensile strength. In polypyrrole(PF_6) used in the experiments presented here, the 50 MPa is the maximum achieved to date. Given the measured strain to charge ratio of $\alpha \sim 1.5\times10^{-10}$ $m^3 \cdot C^{-1}$, the maximum voltage generated is expected to be about 8 mV. In

polyacetylene fibers tensile stresses of 900 MPa are achieved (Baughman and others 1991). Optimistically assuming that the strain to charge ratio remains constant at such high stresses, and that there is little plastic deformation, the maximum voltage that might be expected using existing materials is 0.15 V. Conducting polymer actuators operate at low voltages but involve large charge transfers. Similarly, as generators, the expected voltages are low but charge transfer is high. Piezo-electric generators have the opposite behavior, producing large voltages but transferring very little charge.

8.4 Summary: Diffusive-Elastic Metal

The 'diffusive-elastic metal' model presented aims to describe the observed electro-mechanical response of polypyrrole actuators. At low frequencies, the model predicts a capacitive response, at intermediate frequencies a diffusion limited behavior, and at high frequencies a purely dissipative character, as observed experimentally. Insertion of ions into the polymer occurs in response to changes in dopant concentration at the polymer/electrolyte interface. Polymer charging time is determined by the rate of dopant diffusion within the polymer. Strains are proportional to charge transfer. Finally, the model predicts that electrical energy can be generated from mechanical work input.

The fundamental equations governing diffusive elastic metal behavior are 15 and 16, representing the admittance, and 19, the relationship between strain and charge. These relationships apply in cases where the applied voltage, V is much greater than the product of the stress and strain per unit charge, $V >> V_m = \sigma \cdot \alpha$. The electromechanical conversion efficiency under constant load is given by Equations 42 or 43, both assuming that mechanical energy is not converted back into electrical energy. V_m is predicted to be the

maximum voltage that can be generated through the input of mechanical work. The diffusive-elastic-metal model is the first to quantitatively relate electrical impedance and mechanical response. Before comparing the model with experimental results, further comparisons are made with other impedance models.

8.5 Other Models

A number conducting polymer impedance models (Otero 1997; Della Santa, De Rossi and Mazzoldi 1997; Della Santa, Mazzoldi, Tonci and De Rossi 1997; Pei and Inganas 1992; Ren and Pickup 1995; Kim, Amemiya, Tryk, Hashimoto and Fujishima 1996; Feldberg 1984; Posey and Morozumi 1966; Penner and others 1988; Penner and Martin 1989; Yeu, Nguyen and White 1988; Tanguy, Mermilliod and Hocklet 1987; Amemiya and others 1993; Mazzoldi, Della Santa and De Rossi 1999; Pei and Inganas 1992; Mao, Ochmanska, Paulse and Pickup 1989; Ho, Raistrick and Huggins 1980; Bull, Fan and Bard 1982) and mechanical property models (Otero 1997; Mazzoldi and others 1999; Della Santa and others 1997; Pei and Inganas 1992; Ren and Pickup 1995) have been proposed. Modeling is made more challenging by the diversity of behavior observed in polypyrrole and other conducting polymers. Most obviously, conducting polymers have a continuum of oxidation states, so that they may behave as electrical insulators (Penner and others 1988; Penner and Martin 1989), semi-conductors and 'metals' (Mao and others 1989; Yeu and others 1988; Ho and others 1980; Bull and others 1982; Posey and Morozumi 1966; Tanguy and Hocklet 1987) even in the course of an experiment. Furthermore, the dopants, solvents and temperatures employed during synthesis have a major effect on morphology and conductivity (Bull and others 1982; Ho and others 1980; Tanguy and others 1987; Yeu and others 1988; Posey and Morozumi 1966; Mao and

others 1989; Yamaura, Hagiwara and Iwata 1988; Menon, Yoon, Moses and Heeger 1998; Kohlman and Epstein 1998). Polymers may act as gels, increasing in volume by an order of magnitude in response to a change in oxidation state, or only by a few tenths of a percent, with no solvent incorporation (Baughman, Shacklette and Elsenbaumer 1991). As a result, many models have been proposed, but few predict properties well over more than a limited potential range. Some of the potential model variations are presented, and the behavior they predict noted, so that the validity and uniqueness of the model presented above may be better evaluated.

8.5.1 Admittance/Impedance Models

It is easy to imagine a number of variations on the 'diffusive metal' model presented. So far it is clear that at low frequencies/long times the polymer/electrolyte impedance appears capacitive. At intermediate times, is characteristic of diffusion, and at short times/high frequencies resistance is expected to dominate the cell impedance. A number of candidate models simulate such a response, based on different modes of mass transport, and thermodynamics. Could there be a Nernstian component to the impedance that appears capacitive? Might ions migrate, convect or diffuse through pores in the polymer rather than diffusing through intermolecular spaces, and if so, how do predictions change? Could electronic and not ionic mobility be the rate-limiting factor? Some of the more likely alternatives are presented or discounted, and means of experimental differentiation are revealed.

8.5.1.1 High Frequency Response and Solution Resistance

The modeling of the high frequency behavior of electrochemical cells by circuit resistance is well accepted, and it is common practice to represent the electrolyte as a resistance. If the rates of mass transport in the electrolyte are comparable or slower than those in the polymer, then the model is inappropriate. At very high frequencies, typically > 40 MHz, the apparent resistance of the electrolyte drops as ion travel is no longer retarded by the solvation sphere (Atkins 1990). In the cases dealt with here, the diffusion coefficients in the electrolyte are two orders of magnitude higher than those in the polymer, and the frequencies are well below those at which the reduction in solvation drag becomes relevant[*]. (No such reduction is observed in solution conductivity measurements made over a frequency range of 1 to 10 MHz).

8.5.1.2 Ionic vs. Electronic Mobility

Could the ionic mobility be higher than the electronic conductivity and mobility? Given that the ionic and electronic carriers are equal in number within the polymer, higher ionic mobility will lead to the build-up of ionic charge at the polymer/metal interface at short timescales. In order to produce the conductivities observed in polypyrrole, the dopant mobility would have to be at least four orders of magnitude larger than the typical ionic mobility in liquid propylene carbonate – a situation that is highly unlikely. In conducting polymers with low conductivities, larger ionic than electronic mobility may occur (Penner and others 1988; Penner and Martin 1989; Mao and others 1989).

---

[*] The Debye-Falkenhagen effect.

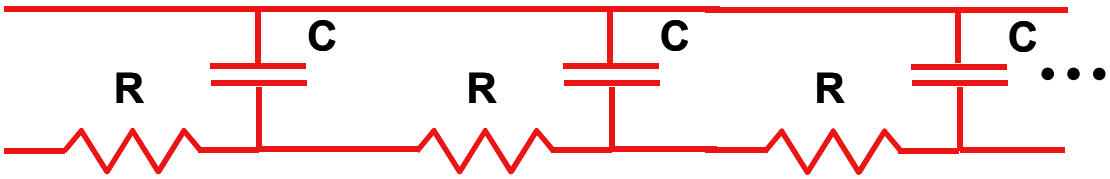

Figure 8.6: Diffusion represented by a transmission line model. The resistors may represent solution resistance, or fluid drag, and the capacitors double layer charging or electrolyte storage.

8.5.1.3 Diffusion, Migration and Porosity

It has been assumed that diffusion is a major rate-limiting factor. As will be seen, the diffusion model appears to describe the observed impedance effectively. However, there are several ways in which a diffusion-like response can arise. One is simply that ions and perhaps some solvent diffuse through the polymer matrix (Penner and others 1988; Penner and Martin 1989; Amemiya and others 1993). A second is that the diffusion occurs mainly within electrolyte filled supermolecular-sized pores inside the polymer (Yeu and others 1988; Tanguy and Hocklet 1987). Finally, migration within a 'porous metal' can be represented by a transmission line model whose equivalent circuit, Figure 8.6, is a solution to the diffusion equation[&] (Posey and Morozumi 1966; Bull and others 1982; Mao and others 1989).

[&] The diffusion time constant for a porous metal is $\tau_D = \frac{S \cdot C \cdot a^2}{\sigma \cdot A}$, where A is the pore cross-section, S is its surface area per until length, C is the capacitance per unit surface area, σ is the electrolyte conductivity and a is the pore length.

There are several means of distinguishing between the possibilities. One is by analyzing cross-sections of the polymer under an electron microscope, and estimating pore sizes. A second is via elemental analysis, in order to determine the relative concentrations of anions, cations, polymer and solvent. If anions are not present in the reduced polymer then there is no electrolyte present. A third is to try various sizes of anions and cations as dopants. If the impedance in the presence of large anions and cations increases much more than their relative diffusion coefficients in liquid electrolyte would suggest, then they likely do not fit into pores, or any pores present are not contiguous. Therefore a pure diffusion model applies, rather than two-phase diffusion or migration models. Finally, the magnitude of the diffusion coefficient may indicate the nature of the mass transport, with high diffusion coefficients ($10^{-9} - 10^{-10}$ $m^2 \cdot s^{-1}$) suggesting the presence of electrolyte within the polymer. Unfortunately, low diffusion coefficients do not necessarily imply the absence of contiguous electrolyte pores within the polymer because pore paths may be tortuous (Yeu and others 1988; Mazzoldi and others 1999).

The fact that polypyrrole, albeit synthesized under different conditions than the material used in this study, is impervious to anions and cations that are beyond a certain dimension, and is useful as a molecular filter (Qiu and Reynolds 1991; Pei and Inganas 1992), is evidence that in many cases the polymer matrix does not contain super-molecular pores that determine mass transport.

Drying of polypyrrole previously soaked in electrolyte or pure propylene carbonate leads to changes in mass of up to 30 %, indicating that there is up to one propylene carbonate molecule present within the polymer per monomer unit. During intake of the solvent the polymer stiffness decreases by a factor of 2. If the bulk of the solvent remains in pores,

then one would expect the engineering modulus (i.e. not accounting for changes in volume upon swelling) to remain constant, but this is not the case.

Finally, the porous metal model suggests that the very large capacitance observed at low frequencies (7×10^7 $F\cdot m^{-3}$ Chapter 7, $5\text{-}40\times10^7$ $F\cdot m^{-3}$ (Arbizzani, Mastragostino and Scrosati 1997; Tanguy and Hocklet 1987; Bull and others 1982; Feldberg 1984)) is due to the charging of an enormous electrolyte/polymer contact area within the polymer. By geometrical arguments, assuming the pore walls possess a typical double layer capacitance of 0.2 $F\cdot m^{-2}$, the average pores are less than 3 nm in diameter. Bearing in mind that the diameters of water, propylene carbonate and hexafluorophosphate ions are roughly 0.26 nm, 0.5 nm, and 0.65 nm respectively, any pores present appear to be at the molecular scale. (Similar arguments and results are found if one assumes that the polymer is inhomogeneous, containing many small regions of high order and high conductivity where surface charging could occur.) The porous metal model and related models, suggest that electric field gradually penetrates pores, increasingly charging their walls as time proceeds. It seems very unlikely that a continuous representation of electrical field lines, as used in the derivation, applies to pores whose sizes are hardly larger than an ion diameter. The results of this calculation suggest that solvent filled pores alone do not account for mass transport and capacitance in polypyrrole employed in this study.

In summary, several observations suggest that migration through electrolyte filled pores, whose surfaces are charged and discharged, does not fully describe polymer behavior. The fact that the engineering elastic modulus decreases by a factor of two upon immersion in propylene carbonate (PC) electrolyte implies that at least some of the

adsorbed PC is plasticizing the polymer by interacting directly with the polymer chains. Secondly, if double layer charging of pores is to account for the observed volumetric capacitance, the pores size is likely to be 3 nm or less. At such a size, roughly 5 propylene carbonate diameters, a continuum model of the electric field distribution is inappropriate. Finally, other researchers have shown, by combined quartz crystal microbalance experiments and cyclic voltammetry (Baker and Reynolds 1988; Pei and Inganas 1992; Qiu and Reynolds 1991), that large ions do not appear to enter polypyrrole.

8.5.1.4 Diffusion vs. Convection

The porous metal model assumes that convection within the pores is negligible. If large pores exist, could they form a circulation system, through which fresh electrolyte is transported, thereby replenishing depleted electrolyte whose ions have been incorporated into the polymer phase? If so, what drives the circulation? De Rossi and his colleagues (Mazzoldi and others 1999; Della Santa and others 1997; Mazzoldi, Degl'Innocenti, Michelucci and De Rossi 1998) include a fluid convection term in their "poro-elastic" model. The rate of fluid flow is assumed to be proportional to a hydrostatic pressure gradient within the polymer, scaled by a fluidic resistance. The pores may become more or less engorged, depending on the direction of fluid flow, creating a fluidic capacitance. Finally, the stress and hence the hydrostatic pressure are assumed to be proportional to charge transferred. The model is only partially solved by De Rossi and colleagues. However, once again a transmission line model applies, Figure 8.7, with fluid storage

capacitance acting in parallel with a fluidic resistance*. In the continuum limit, the process is governed by the diffusion equation. The mathematical form of the response is not sufficient to distinguish between molecular diffusion and fluidic convection mechanisms.

As before, there are a number of ways of deciding between molecular diffusion and electrolyte convection. The arguments presented in the preceding section strongly suggest that contiguous, electrolyte-filled pores are not present within the polymer, and therefore that significant convection is unlikely.

The poro-elastic model is numerical and as yet unsolved, so it is difficult to compare the predictions quantitatively.

8.5.1.5 Kinetics Limited Response

Electrons are transferred to and from the polymer via a metal electrode. Is the rate of electron transfer rate limiting? Are electrons transferred between the polymer and the electrolyte limiting response? Theoretical treatments of kinetics-limited behavior generally begin with the assumption that in order for electrons to be exchanged, the occupation of intermediate electronic states, whose energies are higher than those of the initial and final states, is required. The intermediate states are said to provide an activation barrier, and the probability of overcoming the barrier is given by a Boltzmann distribution. The Butler-Volmer equation predicts that under such circumstances the

---

* The predicted poro-elastic diffusion time constant is $\tau_D = \frac{(1+\nu)\cdot(1-2\cdot\nu)\cdot f\cdot a^2}{\pi^2\cdot E\cdot(1-\nu)}$, where f is the fluidic resistance, and ν is the polymer Poisson ratio.

current is directly proportional to overpotential (the deviation in potential from equilibrium) for small voltage drops (less than about 10 mV), and rises exponentially in voltage at large overpotential (greater than ~ 0.1 V) (Bard and Faulkner 1980) at room temperature. An exponential rise in current as a function of overpotential is thus a strong indication of kinetics-limited behavior.

In Chapters 5 and 10 it is shown that the response to voltage steps and sinusoidal inputs scales linearly with potential over potential ranges from 0.01 to > 1V. These data provide strong evidence that electron transfer kinetics are not a major rate limiting factor.

Another means of testing whether kinetics limit charge transfer at the metal/polymer interface is to pass large currents through a metal/polymer interface, and observed the voltage drop. Four point probe resistance measurements indicate that the metal/polymer interface generally dominates the total resistance, so it is relatively easy to produce large potential drops (tens of volts) across this interface. Even at such high potentials the behavior is ohmic, indicating that kinetics are not significantly rate limiting in the polypyrrole employed. Note that the Ohmic response indicates that the electron transfer is not dominated by Nernstian thermodynamics. On the other hand, pressure and contact area have a large influence on contact resistance, suggesting that the number of metal/polymer electrical contact points limits current at a given voltage.

8.5.1.6 The Thermodynamics: Nernstian vs. Interacting Particles

The Nernst equation describes the thermodynamics of many interactions involving charge transfer. The thermodynamics of polypyrrole charging are described in the diffusive-elastic-metal model by a capacitance, based on observations of the long time/low

frequency response. Can a capacitive response be simulated by a Nernstian allocation of states? In analyzing this question, insight is gained into the nature, though not the precise mechanism, of charge transfer.

The Nernst equation provides a relationship between the population of two states, such as the ratio of concentrations of charged, $[P^+]$, to uncharged, $[P]$, monomer units on the polymer backbone, in terms of applied potential, E, and the relative potential energies of each state, E_o:

$$E - E_o = \frac{R \cdot T}{F} \cdot ln \frac{a \cdot [P^+]}{[P]}, \tag{44}$$

where a is the activity coefficient, F is number of coulombs per mole of fundamental charges, T is temperature and F is the number of coulombs per mole of fundamental charges. Since the concentration of monomers, N, is fixed, $[P^+] + [P] = N$. Capacitance is the change in voltage, E, per unit charge, which is proportional to the change in voltage resulting from a change in concentration of P^+:

$$\frac{\partial E}{\partial [P^+]} = \frac{R \cdot T}{F \cdot [P^+]} - \frac{R \cdot T}{F \cdot (N - [P^+])}\bigg|_{a=const}. \tag{45}$$

The concentration is equal to the charge per unit volume scaled by Avogadro's number, L, and hence Equation 44 describes a Faradaic 'pseudo-capacitance' per unit volume, $\overline{C_F}$:

$$\frac{\partial E}{\partial \rho} = \frac{R \cdot T}{F^2} \cdot \left(\frac{1}{[P^+]} - \frac{1}{N - [P^+]} \right) = \frac{1}{\overline{C_F}} \approx 10^{-10} \frac{\mathrm{V \cdot m^3}}{\mathrm{C^2}}. \tag{46}$$

The value of $\overline{C_F}$ is estimated to be 10^{10} F·m^{-3}. The Faradaic pseudo-capacitance is three orders of magnitude larger than the observed volumetric capacitance. In other words, the real system requires a potential difference that is 1000 × greater than that predicted by the Nernst Equation to achieve the same charge transfer. The Nernst equation similarly predicts that nearly all charge transfer occurs over a roughly 200 mV range of potential about E_o, and that the observed pseudo-capacitance over this range of potentials varies enormously. The response could be a superposition of a number of Nernstian governed charge transfers, but this seems unlikely. Some other mechanism is dominating the energetics of charge transfer.

The Nernst equation assumes that particles do not interact. As the polymer tends from a neutral to a charged state, however, interactions between charges become increasingly strong. These are shielded by the presence of dopants and solvent, but once the concentration becomes sufficiently high the interactions will be important, and may either prevent or encourage charge transfer. Such interactions are disregarded by the Nernst equation. At what level of charge concentration might Nernstian behavior become invalid?

In water, interactions between dissolved ions become significant at concentrations as low as 0.01 M, and dominant above ~0.2 M (Atkins 1990). The concentration of dopants in polypyrrole is roughly 3 M, and is a lower dielectric constant environment than water, so shielding of charges will be lower than in aqueous solution. Thus, based on electrostatic interactions alone, the assumption of non-interacting particles is clearly invalid. Initial

calculations of the magnitude of electrostatic interactions* show that these equal or exceed the expected energies of hydrogen bonding, and therefore play an important role in determining molecular structure. This should not be surprising, as electrostatic interactions are critical in determining the forms and solubilities of many charged polymers, including proteins and DNA.

A review of the literature shows that authors tend to consider the mechanisms of charge transfer Nernstian when the polypyrrole is in its reduced, neutral state (Penner and others 1988; Penner and Martin 1989), and metallic in the oxidized, highly doped state (Bull and others 1982). A number of authors have attempted to describe the transition from neutral to doped states as a superposition of the Nernstian and capacitive behaviors (Mao and others 1989; Feldberg 1984), with the extent of volumetric capacitance being proportional to the charge transferred. A complete thermodynamic description of charge transfer in conducting polymers requires knowledge of the available energy levels and the interaction between them. For the purposes of this study, the capacitive model presented, Equation 15, is taken as sufficient to describe behavior over the range of potentials employed. It seems unlikely that this response is the result of Nernstian behavior.

8.5.2 Models of Electro-Mechanical Coupling

It has been assumed that polymer swelling is due to ion insertion, and thus is likely proportional to ion size plus any entrained solvent. De Rossi and his colleagues

---

* These calculations use techniques developed in solid state physics to explain the cohesion of salts. The relative disorder in polymers makes it difficult to make quantitative predictions, but rough calculations guided by x-ray diffraction data may provide some further insights into the factors, electrostatic and otherwise, that determine polypyrrole molecular structure, and actuation.

(Mazzoldi and others 1999) have proposed an alternative model, in which internal stress is a function of charge. The internal stress in turn leads to a convective flow of electrolyte, resulting in volume changes. This "poro-elastic" model was first used to describe the swelling of gel elastomeric actuators, into which there clearly is a substantial solvent flux. If rate of convection is assumed to determine the impedance, as well as limiting strain rate, then the form of the poro-elastic model cannot be distinguished from the diffusive-elastic metal picture. For reasons described above, it appears that this model does not apply to polypyrrole as synthesized for the studies presented in this thesis.

Attempts have been made to observe changes in molecular structure as a function of doping level (Lee 1999). Unfortunately, changes in structure are too small to be observed by x-ray diffraction, due to the broad diffraction peaks. These result from the relatively small domain sizes in polypyrrole, ~2 nm (Pouget, Oblakowski, Nogami, Albouy, Laridjani, Oh, Min, MacDiarmid, Tsukamoto, Ishiguro and Epstein 1994; Lee 1999; Kohlman and Epstein 1998).

Investigations of strain to charge ratio as a function of dopant size and solvent may provide some insights. However, it is not a straightforward matter to choose appropriate dopants. Factors other than size, such as the presence of hydrophobic side chains, reactions with the polymer and electrochemical degradation of the dopant complicate the experiment (Yamaura, Hagiwara and Iwata 1988). Determination of the strain mechanisms is left to future work.

8.5.3 Model Uniqueness

A number of mechanisms produce a diffusion-like behavior. Comparing model predictions with observed admittances is therefore an insufficient basis on which to determine the mechanism of mass transport. Indications are that mass transport occurs by molecular diffusion through the polymer phase, and not in electrolyte filled pores, but further verification is required.

The molecular origins of the volumetric capacitance and of charge-induced strain remain unclear. However, electrostatics and possibly steric interactions are likely to play a role in both. Work by Pei and colleagues show that direction of charge induced strain depends on whether cations or anions are inserted in order to balance charge, with strain always increasing when dopants are inserted (Pei and Inganas 1993). Their results suggest that ion size may play a role. In Chapter 5 it is shown that solvent also plays a role, with strain to charge ratio doubling when an aqueous electrolyte is used instead of PC.

8.6 Model Variable Evaluation

The diffusive-elastic metal model presented in this chapter, represented by equations 15, 16, and 19, has six independent variables. The strain to charge ratio, α, is experimentally determined via the strain to current transfer function, as are the polymer dimensions. This leaves the electrolyte/contact resistance, R, the diffusion coefficient, D, and the double layer capacitance, C, to be determined. Ideally at least two of these variables can be independently determined.

Electrolyte conductivity can be measured independently. From the cell geometry it is then possible to determine upper and lower bounds on the electrolyte contribution to resistance. The solution resistance can also be measured by passing current between the film and the counter electrode, and measuring the potential drop between the reference electrode and a probe near the film surface. The contact resistance is also measurable, and therefore it is possible to determine R independently.

Unfortunately, apparently due to large diffusion currents which discharge the double layer, it is not a simple matter to measure double layer capacitance, C. Double layer capacitance is expected to be between 0.1-0.4 $F \cdot m^{-2}$ (Bard and Faulkner 1980). It is a function of surface area, the electrolyte, and the electrode surface texture. The volumetric capacitance, however, can be independently measured by, for example, injecting constant current and measuring response, as is done in Chapter 5. The double layer capacitance is then determined from the volumetric capacitance via Equations 16 and 18. It should be possible to measure double layer capacitance directly by placing a reference electrode very close to the polymer surface, thereby reducing double layer charging time to below the minimum diffusion time, τ_C. As discussed in Chapters 9 and 10, very close is likely a few micrometers. Such a measurement would allow the assumption of capacitance per unit volume in the double layer and the polymer to be tested.

There are a number of methods of measuring the diffusion coefficient, D. However, most involve some assumptions about the nature of the double layer, and the modes of ionic and electronic charge transport within the polymer. Nuclear magnetic resonance (NMR) offers an elegant means of determining diffusion coefficients directly from molecular

motions in solids and liquids[$]. So far attempts to measure the diffusion of PF_6^- ions in polypyrrole using NMR have been unsuccessful. Thus, the diffusion coefficient is left as a free parameter. A number of authors have reported diffusion coefficients, or presented data from which diffusion coefficients can be calculated. In polyaniline, values for various ions range between 0.2×10^{-12} and 50×10^{-12} $m^2\cdot s^{-1}$ (Herod and Schlenoff 1993; Kaneko, Fukui, Takashima and Kaneto 1997; Kaneto, Kaneko, Min and MacDiarmid 1995; Kaneto, Kaneko and Takashima 1995), while in polypyrrole diffusion coefficients are reported between 0.02×10^{-12} and 50×10^{-12} $m^2\cdot s^{-1}$ (Penner and others 1988; Penner and Martin 1989; Burgmayer and Murray 1984; Pei and Inganas 1992; Mao and others 1989; Amemiya and others 1993). The values vary greatly, and so only provide very rough bounds on the expected value of D. This variation can be explained by the variety of synthesis techniques, electrolytes, doping levels, and measurement techniques employed. The electrolyte and synthesis conditions that are most similar to those employed in this thesis suggest that $D \sim 1\text{-}20\times10^{-13}$ $m^2\cdot s^{-1}$ (Penner and others 1988; Penner and Martin 1989; Burgmayer and Murray 1984).

[$] In this method, strong pulsed field gradients are used to set nuclear spins rotating at a frequency which is a function of position. After a period of time, T, the pulsed gradient is reapplied to set the spins rotating in the opposite direction, but with the same spatial frequency variation. If the particles being measured have not moved, the spins all realign at time $2\cdot T$. Diffusion leads to a reduction of the signal, which is related to D. Standard techniques are used to account for other (T1, T2) spin loss mechanisms. Of course, the diffusing specied must posses a nuclear moment.

8.7 Conclusion

The electromechanical response of polypyrrole actuators is modeled. Based on empirical evidence, the strain is assumed to be proportional to charge transferred to the polymer, Equation 19. Double layer charging and diffusion limit the rate of charge transfer, Equation 15. The polymer itself is treated as a porous capacitor. The model predicts that polypyrrole may act as a generator, with applied stress creating a voltage proportional to applied load and the strain to charge ratio. Electromechanical conversion efficiencies are also predicted, Equations 42/43.

Other potential models are discussed. It is shown that diffusion in the polymer is the most likely rate limiting factor in the polypyrrole employed, and not diffusion, migration or convection through electrolyte filled pores, as has been suggested by others. Also, models relating charge transfer to the Nernst equation are shown to be inadequate, and it is suggested that in the highly conductive, and oxidized state, electrostatic and other interactions likely dominate the thermodynamics.

Finally, methods are discussed by which the model parameters can be independently determined.

The next chapter describes experimental methods used to measure impedance and strain to charge ratios.

8.8 Reference List

Amemiya, T., Hashimoto, K. and Fujishima, A. Frequency-Resolved Faradaic Processes in Polypyrrole Films Observed by Electromodulation Techniques: Electrochemical Impedance and Color Impedance Spectroscopies. Journal of Physical Chemistry, 1993, 97, 4187-4191.

Arbizzani, Catia; Mastragostino, Marina, and Scrosati, Bruno. Conducting polymers for batteries, supercapacitors and optical devices. Nalwa, Hari Singh, Editor. Handbook of organic and conductive molecules and polymers. Chichester: John Wiley & Sons; 1997; pp. 595-619.

Atkins, P. W. Physical Chemistry. 4 ed. New York: W.H. Freeman; 1990.

Baker, Charles K. and Reynolds, John R. A Quartz Microbalance Study of the Electrosynthesis of Polypyrrole. Journal of Electroanalytical Chemistry, 1988, 251, 307-322.

Bard, Allen J. and Faulkner, Larry R. Electrochemical Methods, Fundamentals and Applications. 1 ed. New York: Wiley; 1980.

Baughman, R. H.; Shacklette, R. L., and Elsenbaumer, R. L. Micro Electromechanical Actuators based on Conducting Polymers. Lazarev, P. I., Editor. Topics in Molecular Organization and Engineering: Molecular Electronics. Dordrecht: Kluwer; 1991a; p. 267.

Bull, Randy A., Fan, Fu-Ren F. and Bard, Allen J. Polymer Films on Electrodes. Journal of the Electrochemical Society, 1982a, 129(5), 1009-1015.

Burgmayer, Paul and Murray, Royce W. Ion Gate Electrodes. Polypyrrole As a Switcheable Ion Conductor Membrane. Journal of Physical Chemistry, 1984a, 88, 2515-2521.

Della Santa, A., De Rossi, D. and Mazzoldi, A. Performance and Work Capacity of Polypyrrole Conducting Polymer Linear Actuator. Synthetic Metals, 1997a, 90, 93-100.

Della Santa, A., DeRossi, D. and Mazzoldi, A. Characterization and Modeling of a Conducting Polymer Mucle-Like Linear Actuator. Smart Materials and Structures, 1997a, 6, 23-34.

Della Santa, A., Mazzoldi, A., Tonci, C. and De Rossi, D. Passive Mechanical Properties of Polypyrrole Films: a Continuum Poroelastic Model. Materials Science and Engineering C, 1997a, 5, 101-109.

Feldberg, Stephen W. Reinterpretation of Polypyrrole Electrochemistry. Consideration of Capacitive Currents in Redox Switching of Conducting Polymers. Journal of the American Chemical Society, 1984a, 106, 4671-4674.

Herod, Timothy E. and Schlenoff, Joseph B. Doping Induced Strain in Polyaniline: Stretchoelectrochemistry. Chemistry of Materials, 1993, 5, 951-955.

Ho, C., Raistrick, I. D. and Huggins, R. A. Application of a-c Techniques to the Study of Lithium Diffusion in Tungsten Trioxide Thin Films. Journal of the Electrochemical Society, 1980a, 127(2), 343-350.

Kaneko, Masamitsu, Fukui, M., Takashima, W. and Kaneto, K. Electrolyte and Strain Dependences of Chemomechanical Deformation of Polyaniline Film. *Synthetic Metals*, 1997a, 84, 795-796.

Kaneto, K., Kaneko, M., Min, Y. and MacDiarmid, Alan G. "Artificial Muscle" : Electromechanical Actuators Using Polyaniline Films. Synthetic Metals, 1995, 71, 2211-2212.

Kaneto, Keiichi, Kaneko, Masamitsu and Takashima, Wataru. Response of Chemomechanical Deformation in Polyaniline Film on Variety of Anions. Japanese Journal of Applied Physics, 1995, 34, Part 2(7A), L837-L840.

Kim, J. J., Amemiya, T., Tryk, D. A., Hashimoto, K. and Fujishima, A. Charge Transport Processes in Electrochemically Deposited Poly(Pyrrole) and Poly(N-Methylpyrrole) Thin Films. JOURNAL OF ELECTROANALYTICAL CHEMISTRY , 1996 Nov 1, 416(1-2), 113-119 .

Kohlman, R. S. and Epstein, Arthur J. Insulator-metal transistion and inhomogeneous metallic state in conducting polymers. Skotheim, Terje A.; Elsenbaumer, Ronald L., and Reynolds, John R., Editors. Handbook of Conducting Polymers. 2nd ed. New York: Marcel Dekker; 1998a; pp. 85-122.

Lee, Yun-Ju. X-ray Diffraction Studies of Polypyrrole. MIT Materials Science and Engineering Undergraduate Thesis. Cambridge, MA; 1999.

Madden, John D. and Hunter, Ian W. Conducting Polymer Actuators: Modeling Efficiency and Frequency Response. Sensors and Actuators, 2000.

Mao, Huanyu, Ochmanska, Jolanta, Paulse, Chris D. and Pickup, Peter G. Ion Transport in Pyrrole-Based Polymer Films. Faraday Discussions of the Chemical Society, 1989a, 88, 165-176.

Mazzoldi, A., Degl'Innocenti, C., Michelucci, M. and De Rossi, D. Actuative Properties

of Polyaniline Fibers Under Electrochemical Stimulation. Materials Science and Engineering C, 1998, 6, 65-72.

Mazzoldi, A.; Della Santa, A., and De Rossi, D. Conducting polymer actuators: Properties and modeling. Osada, Yoshihito and De Rossi, Danilo E., editors. Polymer Sensors and Actuators. Heidelberg: Springer Verlag; 1999.

Menon, Reghu; Yoon, C. O.; Moses, D., and Heeger, A. J. Metal-insulator transition in doped conducting polymers. Skotheim, Terje A.; Elsenbaumer, Ronald L., and Reynolds, John R., Editors. Handbook of Conducting Polymers. 2nd ed. New York: Marcel Dekker; 1998; pp. 27-84.

Nogami, Yoshio, Pouget, Jean-Paul and Ishiguro, Takehiro. Structure of Highly Conducting PF_6^--Doped Polypyrrole. Synthetic Metals, 1994, 62, 257-263.

Otero, Toribio Fernandez. Artificial Muscles, electrodissolutoin and redox processes in conducting polymers. Nalwa, Hari Singh, Editor. Handbook of organic and conductive molecules and polymers. Chichester: John Wiley & Sons; 1997; pp. 517-594.

Pei, Qibing and Inganas, Olle. Electrochemical Application of the Bending Beam Method. 1. Mass Transport and Volume Changes in Polypyrrole During Redox. Journal of Physical Chemistry, 1992a, 96(25), 10507-10514.

---. Electrochemical Applications of the Beam Bending Method; a Novel Way to Study Ion Transport in Electroactive Polymers. Solid State Ionics, 1993, 60, 161-166.

Penner, Reginald M. and Martin, Charles R. Electrochemical Investigations of Electronically Conductive Polymers. 2. Evaluation of Charge-Transport Rates in Polypyrrole Using an Alternating Current Impedance Method. Journal of Physical Chemistry, 1989a, 93, 984-989.

Penner, Reginald M.; Van Dyke, Leon S., and Martin, Charles R. Electrochemical Evaluation of Charge-Transport Rates in Polypyrrole. 1988a; 92, 5274-5282.

Posey, F. A. and Morozumi, T. Theory of potentiostatic and galvanostatic charging of the double layer in poirous electrodes. 1966a; 113, (2): 176-184.

Pouget, J. P., Oblakowski, Z., Nogami, Y., Albouy, P. A., Laridjani, M., Oh, E. J., Min, Y., MacDiarmid, A. G., Tsukamoto, J., Ishiguro, T. and Epstein, A. J. Recent Structural Investigations of Metallic Polymers. Synthetic Metals, 1994, 65, 131-140.

Qiu, Yong-Jian and Reynolds, John R. Dopant Anion Controlled Ion Transport Behvior of Polypyrrole. Polymer Engineering and Science, 1991a, 31, 417-421.

Ren, X. M. and Pickup, P. G. Impedance Measurements of Ionic Conductivity As a Probe of Structure in Electrochemically Deposited Polypyrrole Films. Journal of

Electroanalytical Chemistry , 1995 Oct 31, 396(1-2), 359-364 .

Tanguy, J. and Hocklet, M. Capacitive Charge and Noncapacitive Charge in Conducting Polymer Electrodes. Journal of the Electrochemical Society: Electrochemical Science and Technology, 1987 Apr, 795-801.

Yamaura, M., Hagiwara, T. and Iwata, K. Ehancement of Electrical Conductivity of Polypyrrole Film by Stretching: Counter Ion Effect. Synthetic Metals, 1988a, 26, 209-224.

Yeu, Taewhan, Nguyen, Trung V. and White, Ralph E. A Mathematical Model for Predicting Cyclic Voltammograms of Electrically Conductive Polypyrrole. Journal of the Electrochemical Society: Electrochemical Science and Technology, 1988a Aug, 1971-1976.